AMMRC TR 85-15

SELF-PROPAGATING REACTIONS FOR SYNTHESIS OF HIGH TEMPERATURE MATERIALS

June 1985

PETER D. ZAVITSANOS and JOSEPH F. D'ANDREA
General Electric Company
Re-Entry Systems Operations
3198 Chestnut Street
Philadelphia, Pennsylvania 19101

FINAL REPORT

Contract No. DAAG46-83-C-0178

Prepared for

ARMY MATERIALS AND MECHANICS RESEARCH CENTER
Watertown, Massachusetts 02172-0001

UNCLASSIFIED

SECURITY CLASSIFICATION OF THIS PAGE (When Data Entered)

REPORT DOCUMENTATION PAGE	READ INSTRUCTIONS BEFORE COMPLETING FORM
1. REPORT NUMBER: AMMRC TR 85-15	2. GOVT ACCESSION NO.: AD-A159 869
3. RECIPIENT'S CATALOG NUMBER:	
4. TITLE (and Subtitle): SELF-PROPAGATING REACTIONS FOR SYNTHESIS OF HIGH TEMPERATURE MATERIALS	5. TYPE OF REPORT & PERIOD COVERED: Final Report - Oct. 83 to Sept. 84
	6. PERFORMING ORG. REPORT NUMBER:
7. AUTHOR(s): Peter D. Zavitsanos and Joseph F. D'Andrea	8. CONTRACT OR GRANT NUMBER(s): DAAG46-83-C-0178
9. PERFORMING ORGANIZATION NAME AND ADDRESS: General Electric Co., Re-Entry Systems Operations, 3198 Chestnut Street, Philadelphia, Pennsylvania 19101	10. PROGRAM ELEMENT, PROJECT, TASK AREA & WORK UNIT NUMBERS: D/A Project: 1L263102D071
11. CONTROLLING OFFICE NAME AND ADDRESS: Army Materials and Mechanics Research Center ATTN: AMXMR-K Watertown, Massachusetts 02172-0001	12. REPORT DATE: June 1985
	13. NUMBER OF PAGES: 93
14. MONITORING AGENCY NAME & ADDRESS(if different from Controlling Office)	15. SECURITY CLASS. (of this report): Unclassified
	15a. DECLASSIFICATION/DOWNGRADING SCHEDULE:

16. DISTRIBUTION STATEMENT (of this Report)

Approved for public release; distribution unlimited.

17. DISTRIBUTION STATEMENT (of the abstract entered in Block 20, if different from Report)

18. SUPPLEMENTARY NOTES

19. KEY WORDS (Continue on reverse side if necessary and identify by block number)

Titanium powder	Synthesis	Exothermic reactions
Boron powder	Heat of reaction	Titanium boride
Titanium diboride	Density	

20. ABSTRACT (Continue on reverse side if necessary and identify by block number)

(SEE REVERSE SIDE)

DD FORM 1 JAN 73 1473 EDITION OF 1 NOV 65 IS OBSOLETE

UNCLASSIFIED

SECURITY CLASSIFICATION OF THIS PAGE (When Data Entered)

Block No. 20

ABSTRACT

This effort was undertaken to investigate the basic aspects of the condensed phase titanium-boron reaction leading to the formation of high density and quality TiB_2 under self-propagating conditions. Candidate factors for controlling microstructure were addressed and were utilized as variables in series of runs which produced TiB_2.

The heat of formation of TiB_2 was measured directly from the reacting elements in a modified bomb calorimeter; a $\Delta H^\circ_{f,298} = -71.81 \pm 1.9$ was determined which is sufficient to produce liquid TiB_2 under adiabatic conditions.

High density titanium diboride was prepared from elemental powders of titanium and boron through the self-propagation reaction process. By applying external pressure during the reaction period the product (TiB_2) has been densified to 95-97% theoretical density.

The microstructure and properties such as density, grain size, hardness, strength, toughness by indentation and modulus by elastic and sonic methods, are discussed as a function of variables such as starting stoichiometry, powder-particle size, mixing techniques and nucleation additives such as TiB_2 powder.

ACKNOWLEDGMENTS

The contributions of the following individuals to the successful completion of this program are gratefully acknowledged.

The genuine technical interest and contributions of Mr. Philip Wong to the physical and microstructure property measurements.

The insights of Dr. Richard Tressler to the micromechanisms of the reaction pressing process and the critical evaluation of physical property results and measurement technology.

The continuous efforts of Dr. Earl Feingold in elucidating experimental results by microanalytical techniques of x-ray and electron microprobe measurements.

The application of specialized test techniques and property data evaluation by John Roetling in development of the physical property data base for TiB_2 by reaction pressing.

The insights of Gerald Dodds for inclusion of the specialized power preparation techniques of jet-milling in this program and other critical contributions in powder processing.

The efforts of Marty Birenbaum in the development of metallographic specimen preparation of the very hard material, TiB_2, which resulted in artifact-free microstructure sections.

TABLE OF CONTENTS

TABLE OF CONTENTS (CONT'D)

LIST OF ILLUSTRATIONS

LIST OF ILLUSTRATIONS (CONT'D)

LIST OF TABLES

1.0 INTRODUCTION AND OBJECTIVES

The use of self-propagating reactions in forming high purity refractory compounds has been explored by the Soviets over a period of several years with some success in forming cost effective abrasive powders. The formation of a densified shape of TiB_2 by applying only pressure during the exothermic self-propagating reaction was first demonstrated by Zavitsanos and Morris[1] where TiB_2 discs were formulated with a density of 96.7% theoretical.

The advantages of self-propagating processes can be many including higher purity, strength, toughness and perhaps production cost. This program was undertaken in an effort to investigate the fundamental aspects of the self-propagating reaction between Ti and B powders leading to the highly exothermic formation of TiB_2, i.e. $Ti(c) + 2B(c) \rightarrow TiB_2(c) + \Delta H$ as well as produce specimens of modest dimensions in order to obtain engineering physical properties leading to an eventual process scale-up utilizing commercially available elemental powders.

The objective of the program was to identify the mechanism of the reaction and identify the most promising conditions leading to highest purity, density and toughness; the suggested candidate factors controlling microstructure and density are the following:

1. Starting reactant powders: purity and size distribution.
2. Powder mixing: ratio, uniformity, seeding.
3. Reaction initiation: point source (hot wire at 900°C); volume heating by furnace to 900°C.
4. Pressure: magnitude and method of application.

---

(1) "Synthesis of Titanium Diboride by a Self-Propagating Reaction", by P.D. Zavitsanos and J.R. MOrris, Jr., Ceramic Eng. and Sci. Proc., July-August 1983, pp. 624-633.

Most of the suggested variables were addressed in the course of the program and high purity samples of titanium diboride were synthesized in the form of wafers (1.75" dia. x 1.25" thick) using the high temperature self-propagating reaction process. Extensive characterization of the samples resulted in increased confidence in terms of proceeding with a cost effective scale-up effort and eventual field tests. The scale-up effort will be based on the effective transfer of the process technology developed on this program to large scale equipment such as high pressure/large volume autoclave.

2.0 THERMOCHEMISTRY

2.1 Heat of Reaction Measurements by Bomb Calorimetry

The heat of formation of TiB_2 as reported in the JANAF Tables[2] is in serious dispute with values ranging from -50 $\pm$ 5 kcal/mole to 73.6 $\pm$ 4.5 kcal/mole. The significance of this problem in the self-propagation synthesis technique is that the lower value of the heat of formation would not be sufficient to produce a liquid TiB_2 product which may play a key role in the densification step. For this reason it was considered necessary to measure the heat of formation by a "direct" method as compared to the JANAF values which were all "indirect."

An automatic adiabatic Bomb Calorimeter (Parr Instrument Co. Model 1291) was used to measure the heat of the reaction $Ti + 2B \rightarrow TiB_2 + \Delta H$. An attempt was also made to measure $2Ti + B_4C \rightarrow 2TiB_2 + C$ but this was not possible under the existing experimental conditions. However the ΔH of several $Ti/2B$, $2Ti/B_4C$ mixtures was possible to be measured.

The Parr bomb calorimeter consists of a sealed stainless steel reaction vessel ("bomb") immersed in a constant temperature water bath. The bomb is equipped with two electrical feedthroughs, a valve to pressurize the bomb, and a vent valve. Reactants are held in a small steel cup suspended in the bomb. A thin fusible wire above the cup is connected to the electrical feed posts. A power supply attached to these posts serves to melt the fuse wire onto the reactants and thus trigger the exothermic reaction. The resulting temperature increase is used to calculate the ΔH for the reaction. A system calibration provides the necessary conversion calories/degree temperature

---

(2) JANAF Thermochemical Data, Dow Chemical Company, Midland, Michigan

rise. The calibration is determined from a standard material of known heat output (Benzoic Acid).

The Ti/B reaction was studied under several conditions of applied atmosphere (air and N_2) using two sources of boron, elemental B and B_4C. Further details of experimental conditions and the resulting heat ($\Delta H^\circ_{f,298}$) are shown in Table I. The results suggest the reaction is so fast that surface heterogeneous reaction(s) with oxygen and/or nitrogen play an insignificant role in the observed heat release which is 1,033 cal/g (or 71.81 kcal/mole) for the Ti/2B mixture and considerably less when the source of boron is B_4C instead of B.

Table II shows the results of this work in comparison with all the JANAF values, and supports the view that an adequate amount of energy is released to raise the (adiabatic) temperature of the product above the melting point of TiB_2 which is 3,003°K.

TABLE I

PARR BOMB HEAT OF REACTION DATA SUMMARY

SAMPLE COMPOSITION			SAMPLE WT. (g)	$\Delta H^{\circ}_{f,298}$ (cal/g)	ATMOSPHERE
Ti + 2B	2Ti + B_4C				
100% (WT)	---	POWDER	5.49	1087	AIR + N_2*
100	---	PELLET	5.70	1037	N_2+
100	---	POWDER	4.38	994	N_2+
100	---	POWDER$^{\Delta}$	6.06	1004	N_2+
100	---	POWDER$^{\Delta}$	5.97	1044 / 1033 AVG	N_2+
70	30	POWDER	4.85	854	N_2+
50	50	POWDER	5.93	744	N_2+
50	50	POWDER$^{\Delta}$	5.91	784 } 764 AVG	N_2+
--	100	DID NOT IGNITE			N_2+

* AMBIENT AIR IN BOMB PRESSURIZED TO 20 PSIG WITH N_2

+ PARR BOMB PURGED WITH N_2 THEN PRESSURIZED TO 20 PSIG

$^{\Delta}$ PREPARED FROM BALL MILLED POWDERS

TABLE II

THERMOCHEMISTRY

$$Ti(s) + 2B(s) \longrightarrow TiB_2(s) = \Delta H$$

$\Delta H^{\circ}_{f,298}$(kcal/mole)	SOURCE	METHOD
-66.85 ± 2.7	JANAF	INDIRECT
-50 ± 5	"	"
-73.6 ± 4.5	"	"
-63.6 ± 2.0	"	"
-67.5 ± 3.5	"	"
71.81 ± 1.9	THIS WORK	DIRECT BOMB CALORIMETRY

3.0 SYNTHESIS PROCESS

3.1 Experiment Definition

The experimental matrix for the synthesis of dense TiB_2 by the self-propagating, high temperature reaction of pre-compacted elemental powder mixes contained in a graphite die system is shown in Table III. The boron powder size effect was examined using nominal powder sizes of 249 μm (-60 mesh), 43 μm(-325 mesh), 10-100 μm (reported as 320Å in error), and 0.150 μm (sub-micron). These boron powders were combined with two titanium powder sizes, 43 μm (-325 mesh) and 1-5 μm as indicated in Table III.

Stoichiometric and off-stoichiometric powder mix compositions were prepared and made into dense compacts by two reaction press processes, denoted as programs #1 and #9 in Table III. In addition, stoichiometric powder mixes using boron carbide (B_4C) as the boron source, and added TiB_2 in the powder mix as a seedant addition were processed. Two pressings, using a jet-milled powder mix were prepared to assess pre-process powder preparation effects.

3.2 Powder Evaluation

The examination of the powders used in the reaction pressing experiments included mass spectrometry on individual powder samples of Ti and B, and scanning electron microscope/energy dispersive x-ray microanalysis (SEM/EDX) on both individual powders and on unreacted powder mixes of Ti + 2B.

TABLE III

EXPERIMENTAL MATRIX FOR TITANIUM DIBORIDE SYNTHESIS BY SPHTS (REACTION PRESSING)

MIX #	COMPOSITION	TITANIUM[1]	BORON[1]	OTHER[1]	EVALUATION CRITERIA	HP #	PROGRAM[2]
3	STOICHIOMETRIC	AEE -325	CALLERY 320A	---	BORON SIZE EFFECT WITH -325 Ti	226	1
3A	STOICHIOMETRIC	ALFA -325	CALLERY 320A	---		187	M
4	2 W/O EXCESS B	AEE -325	CALLERY 320A	---	OFF-STOICHIOMETRY EFFECT	228	1
6	STOICHIOMETRIC	AEE -325	AEE -325	---	BORON SIZE EFFECT WITH -325 Ti	214	1
7	STOICHIOMETRIC	AEE -325	ALFA -60	---		211, 215	1
8	STOICHIOMETRIC	AEE 1-5 μm	CALLERY 320A	---	BORON SIZE EFFECT WITH 1-5 μm Ti	212	1
9	STOICHIOMETRIC	AEE 1-5 μm	AEE -325	---		213	1
10	STOICHIOMETRIC	AEE 1-5 μm	ALFA -60	---		230	1
11	STOICHIOMETRIC	ALFA -325	---	AEE B_4C 1-5 μm	CARBIDE AS BORON SOURCE	186, 231	M,1
--	STOICHIOMETRIC, WITH MIXED BORON POWDERS	AEE -325	AEE -325 AND CALLERY SUB-MICRON	---	MIXED BORON SIZE EFFECT WITH -325 Ti	277, 278	1
--	5 W/O EXCESS Ti	AEE -325	AEE -325	---	OFF-STOICHIOMETRY EFFECT	286, 287	9
--	7.5 W/O EXCESS Ti	AEE -325	AEE -325	---	OFF-STOICHIOMETRY EFFECT	288, 289	9
--	STOICHIOMETRIC, JET-MILLED POWDER MIX	AEE -325	AEE -325	---	POWDER PREPARATION EFFECT	303	9
--	STOICHIOMETRIC, JET-MILLED, 1 W/O ADDED TiB_2	AEE -325	AEE -325	AEE TiB_2 1-5 μm	SEEDANT ADDITION	304	9

(1) MESH OR PARTICLE SIZE AS REPORTED BY SUPPLIER
- (a) -325 EQUIVALENT TO 0.0017" (43 μm)
- (b) -60 EQUIVALENT TO 0.0098" (249 μm)
- (c) CALLERY 320A REPORTED BY SUPPLIER IN ERROR; SEM MEASUREMENTS ≈ 10 μm IN SMALLEST DIMENSION OF PARTICLE AND ≈ 100 μm IN LARGEST DIMENSION
- (d) CALLERY SUB-MICRON = 1500A MEAN, EQUIVALENT TO 0.150 μm

(2) PROGRAM M, HP187 = 90 MINUTE RAMP TO 1750°C, 30 MINUTE HOLD AT 1750°C
HP186 = 80 MINUTE RAMP TO 2000°C, 20 MINUTE HOLD AT 2000°C
PROGRAM 1, 15 MINUTE HOLD AT 1040°C, 50 MINUTE HOLD AT 1760°C
PROGRAM 9, 60 MINUTE RAMP TO 1760°C, 60 MINUTE

3.2.1 Mass Spectrometry

Time of flight mass spectrometric measurements were made on volatile products from two sources of boron (Callery and Atlantic Equipment Engineers (AEE)) and two sources of titanium (AEE and Alfa Products). This was done to detect any significant adsorbates or impurities between sources of the two powder materials used to fabricate TiB_2 that might account for differences in behavior during formation. Both titanium samples showed hydrogen evolving above about 1600°C, while the Alfa material showed somewhat more carbon and oxygen species as well as a higher total volatile content as evident by the total mass spectrometer signal.

Both boron specimens gave identical responses relative to mass number, but the Callery specimen gave about 30% more total counts due mainly to mass numbers 44 and 45. A summary of data is given in Table IV. Inasmuch as the prior history of the materials as well as the processes by which they were made are not completely known, it is not possible to assign chemical compound formulas to all mass numbers observed in the analyses. Yet some possibilities are listed in Table IV mainly resulting from the presence of carbon, oxygen, hydrogen and/or water vapor adsorbed on the powder surfaces.

3.2.2 SEM/EDX Evaluation

The suppliers and the powder descriptions are shown in Table V. Figures 1 and 2 illustrate the individual powder morphology for AEE -325 mesh Ti and for AEE -325 mesh B. These powders, when combined in solids-solids mixed stoichiometric and excess Ti formulas, obtained consistent density and strength properties when reaction pressing processed. The jet-milled, stoichiometric composition of these powders obtained the best flexure strength properties for that powder combination.

TABLE IV

SUMMARY OF MASS SPECTROMETRY RESULTS, TOTAL COUNTS TO 1800°C

	TITANIUM POWDERS			BORON POWDERS	
MASS NO.	POSSIBLE SPECIES	AEE Ti	ALFA Ti	POSSIBLE SPECIES	CALLERY B	AEE B
1	H		370			
2	H_2	7640	7730	H_2	1350	760
11				B	480	200
12	C		10620	B H,	200	590
15	CH_3		5250			
16	O	1300	9890			
20	--	3750		--	2770	2360
36	--	1070		--	3130	150
44	CO_2	3250		CO_2	6010	1950
45				H_2B O_2	4250	2550
47				--	5090	6900
48	Ti	3100	5250			
49				--	3350	5020
65				--		600
83				--	250	
TOTAL (COUNTS)		20110	38740		26880	21080

TABLE V

SUPPLIER POWDER DESCRIPTION

MATERIAL	SUPPLIER POWDER DESCRIPTION	SUPPLIER[1]	SEM/EDX EXAMINATION
TITANIUM	-325 MESH; 99% METAL PURITY; PACKED UNDER ARGON	ALFA	ALFA -325 Ti + CALLERY SUB-MICRON B; (FIGURE 8)
	-325 MESH; 99.7%	AEE	AEE -325 Ti (FIGURE 1); AEE -325 Ti + AEE -325 B (FIGURE 2)
	1-5 MICRON; 99.7%	AEE	AEE 1-5 Ti + AEE -325 B (FIGURE 4)
BORON	-60 MESH CRYSTALLINE; 99.7% METAL PURITY, 99.4% TOTAL PURITY	ALFA	ALFA -60 B + AEE -325 Ti (FIGURE 6)
	-325 MESH CRYSTALLINE; 99.5% MIN. PURITY	AEE	AEE -325 B (FIGURE 2); AEE -325 B + AEE -325 Ti (FIGURE 3)
	SUB-MICRON, HIGH PURITY; 99.9%	CALLERY	CALLERY SUB-MICRON B + ALFA -325 Ti (FIGURE 8)
	320 ANGSTROM; PACKED UNDER NITROGEN	CALLERY	CALLERY 320 B + AEE 1-5 Ti (FIGURE 7)
BORON CARBIDE	1-5 MICRON; 99.7%	AEE	NONE
TITANIUM DIBORIDE	1-5 MICRON; 99.8%	AEE	NONE

(1) ALFA = ALFA PRODUCTS, DANVERS, MASSACHUSETTS
AEE = ATLANTIC EQUIPMENT ENGINEERS, BERGENFIELD, NEW JERSEY
CALLERY = CALLERY CHEMICAL CO., CALLERY, PENNSYLVANIA

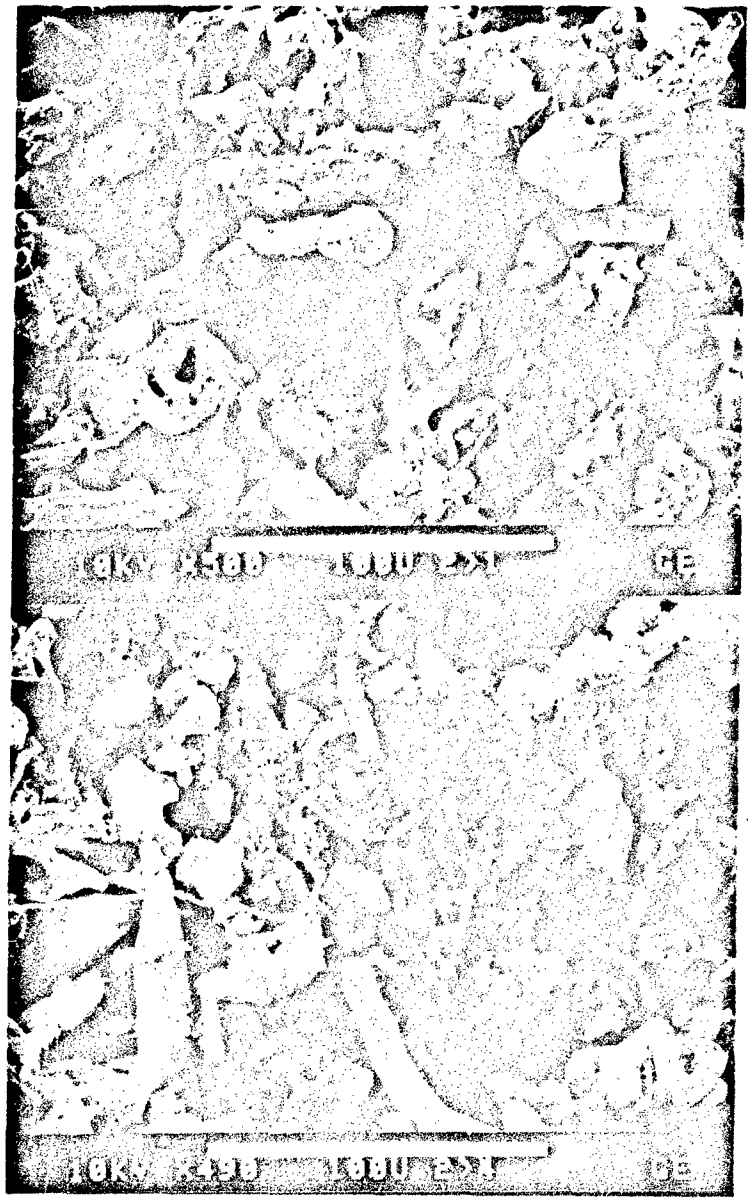

Figure 1. SEM examination of AEE -325 mesh Titanium from two different powder lots.

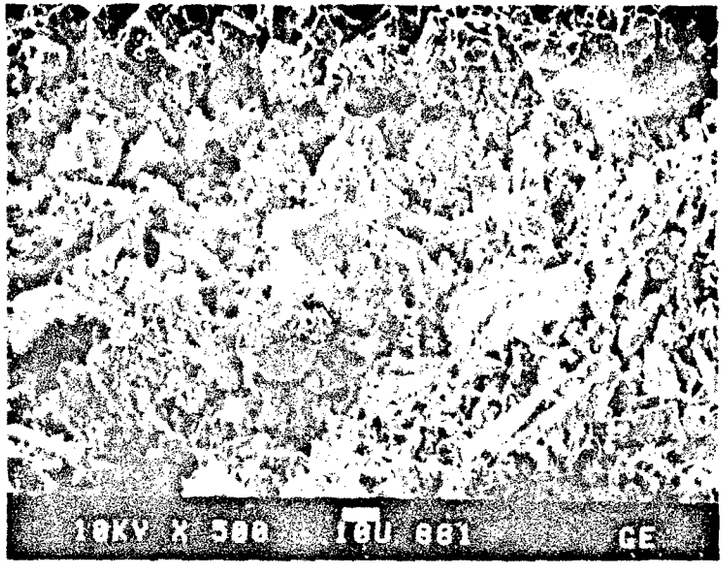

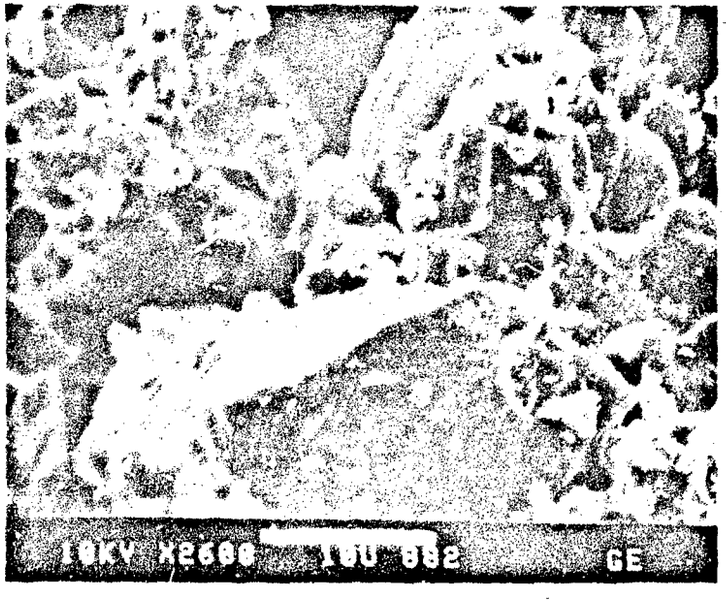

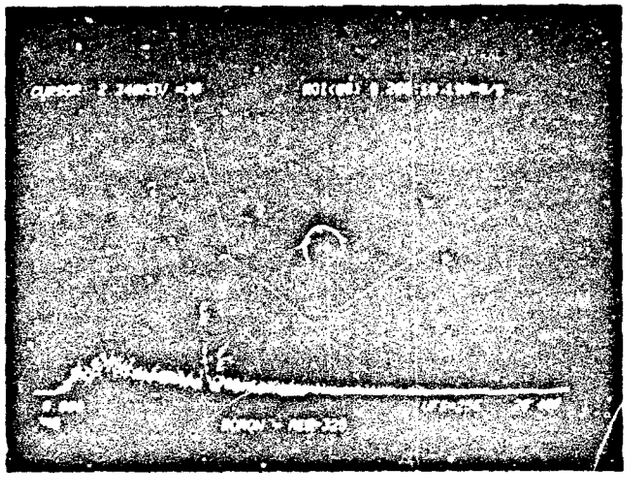

Figure 2 . SEM/EDX examination of AEE -325 mesh boron.

Green compacts, representing the various combinations of four boron powder sizes with two titanium powder sizes, were prepared and the fracture surfaces of these unreacted powder mixes were examined, Figures 3 thru 8. This qualitative examination of the powder particle morphology suggests that the Ti powders have a wide particle size distribution, angular and elongated particle shapes, and a high degree of aggregation.

Similar observations apply to the larger boron powders (-325 and -60 mesh), whereas these comments are not valid for the sub-micron boron (Fig. 8) because of the difficulty of resolving the individual particles. The Callery boron, originally identified by Callery Chemical Co. as "320 angstrom" mean particle size, was an in-house supply used in early experimentation. Figure 7 indicates that the powder had a thin lamallae morphology suggesting a parallel growth habit[3,4] with possible interpenetration twin growths which is expected in crystal growth from a vapor phase reaction or decomposition. Measurements of the angular crystal faces suggest this boron powder is the low temperature (800°C - 1100°C) α-rhombohedral form.[5]

---

(3) An Introduction to Crystallography, F.C. Phillips, Longmans Green and Co. Ltd., 1965.

(4) Crystallography and Crystal Defects, A. Kelly and G.W. Groves, Addison-Wesley Pub. Co., 1970.

(5) Structure and Polymorphism in Elemental Boron, J.L. Hoard; and Preparation and Chemistry of Elementary Boron, A.E. Newhi, both in Borax to Boranes, Advances in Chemistry Series No. 32, American Chemical Society, 1961.

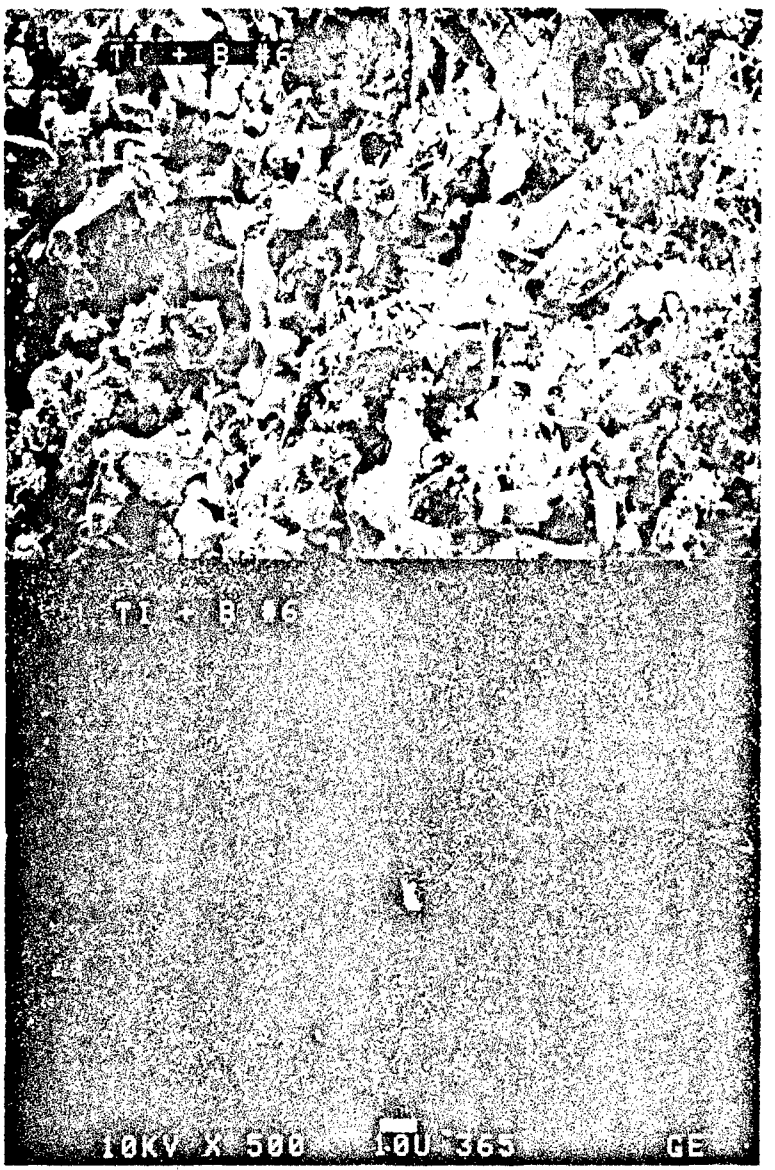

Figure 3. Fracture surface of green compact of Ti + B Mix #6 stoichiometric Ti + 2B, AEE -325 mesh titanium + AEE -325 mesh boron. Top, SEM photomicrograph of particle shapes and sizes. Bottom, Ti x-ray map of same area.

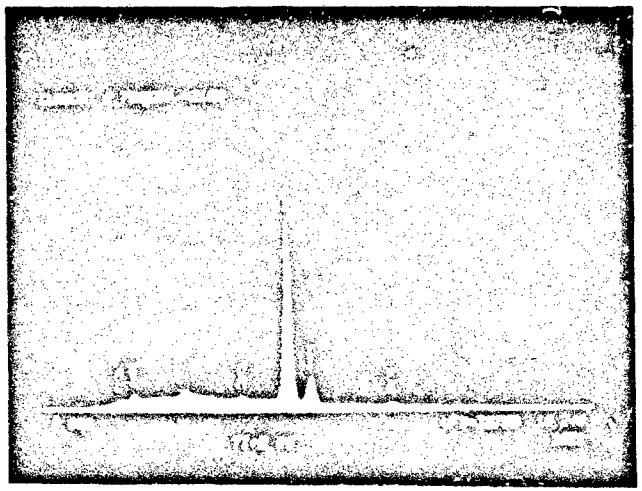

Figure 4. SEM/EDX examination of green compact of stoichiometric T + 2B, AEE 1-5 micron titanium + AEE -325 mesh boron.
Left: SEM image and titanium x-ray map of identical areas.
Top: X-ray energy spectra of powder mix.

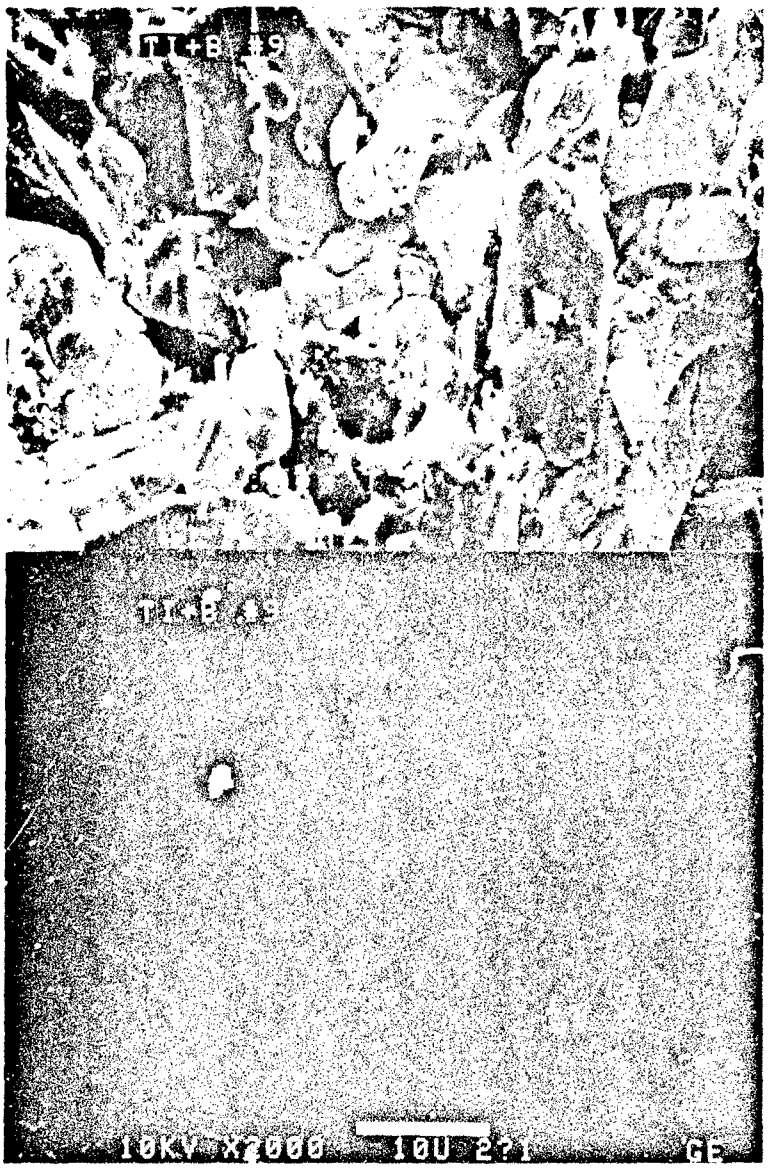

Figure 5. SEM examination of green compact of stoichiometric Ti + 2B, AEE 1-5 micron titanium + AEE -325 mesh boron. Top: SEM image; Bottom; Titanium x-ray map of identical area.

Figure 6. Fracture surface of green compact of stoichiometric Ti + 2B, AEE -325 mesh titanium + Alfa -60 mesh boron. Top: SEM photomicrograph illustrating particle shapes and sizes. Bottom: Ti x-ray map of same area.

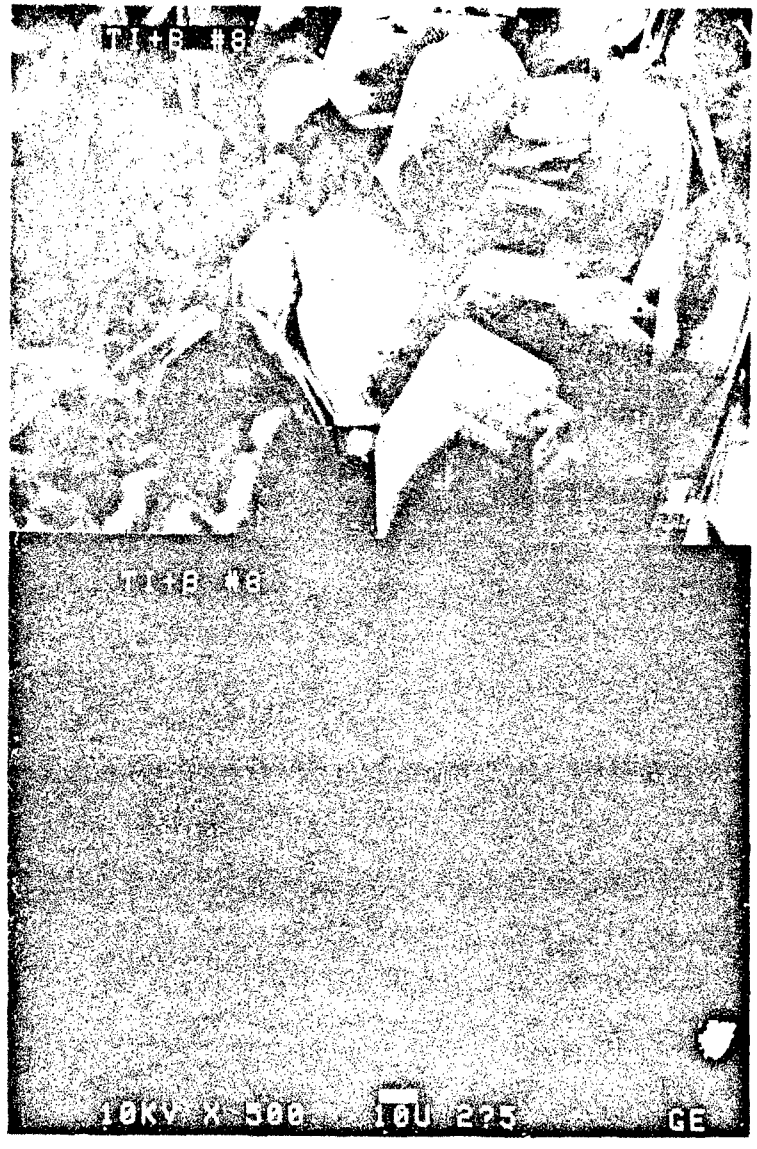

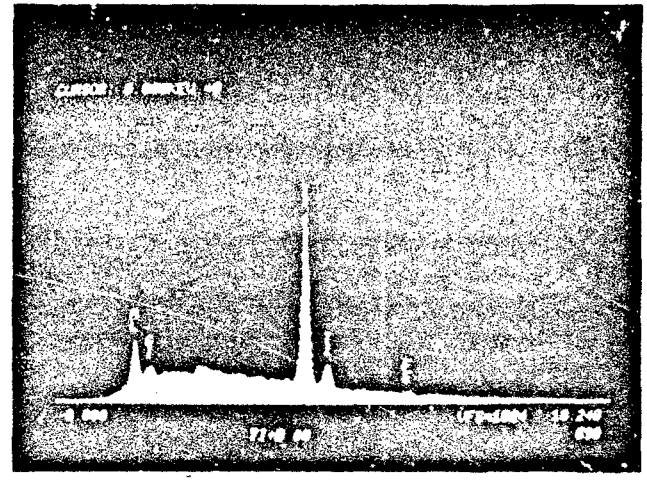

Figure 7. SEM/EDX examination of green compact fracture of stoichiometric Ti + 2B, AEE 1-5 micron titanium + Callery 320Å boron.
Left: Detail of powder particle morphology and agglomeration with Ti x-ray of same area.
Top: X-ray spectra of powder mix.

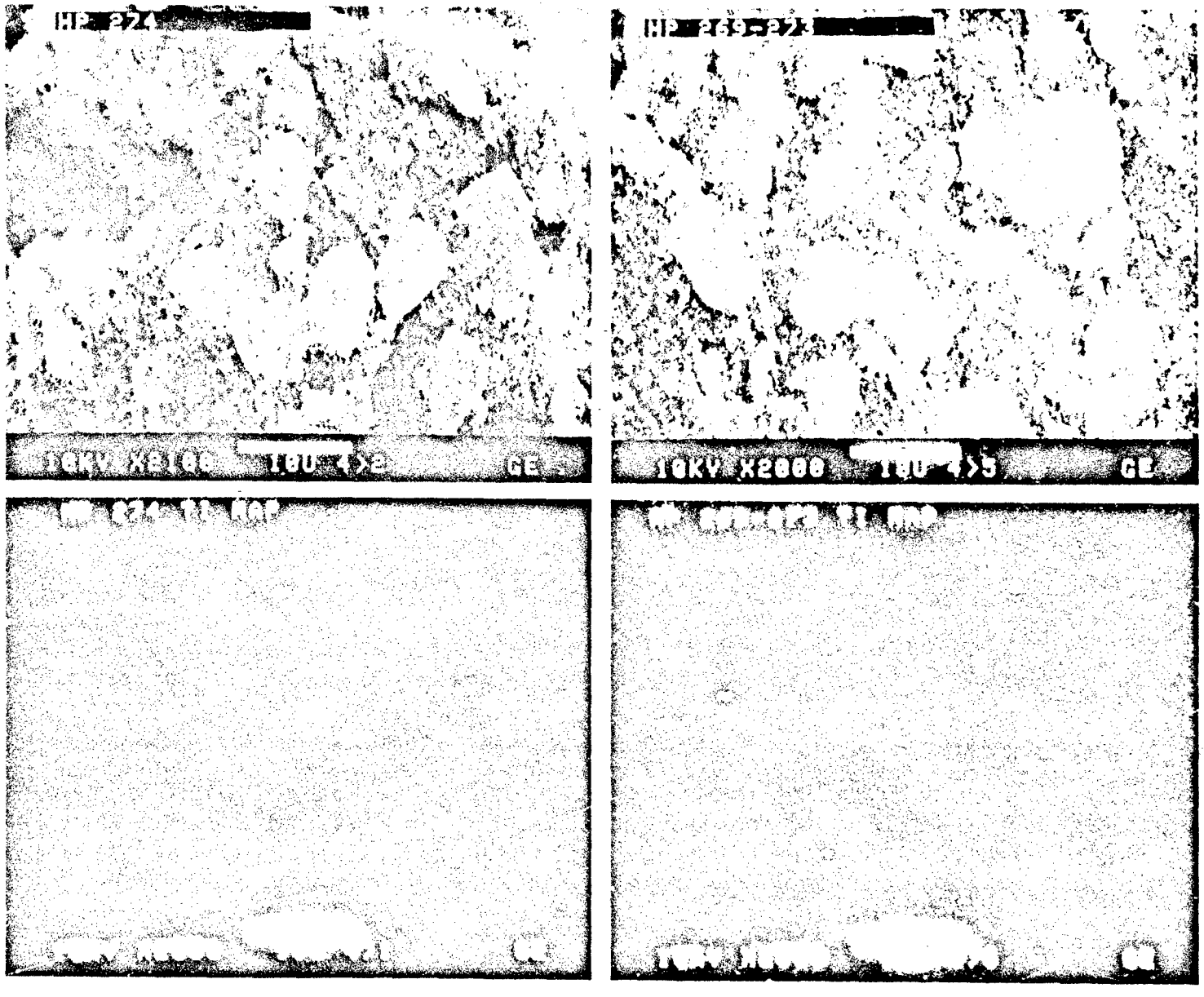

Figure 8. SEM examination of powder mix: Alfa -325 mesh Titanium + Callery Sub-micron Boron. (This combination resulted in uncontrolled reaction during pressing.)

EDX spectra are presented for AEE -325 mesh B (Fig. 2), AEE 1-5 micron Ti + AEE -325 mesh B (Fig. 4), and AEE 1-5 micron Ti + Callery 320Å (Fig. 7). The boron powder spectra indicates a trace[6] of Fe, and the powder mix analysis shows traces Fe, Si, Al, and Ca.

3.3 Powder Mixing

Jar milling, solids-solids blending, and jet milling techniques were attempted for powder mixing of 40 g to 100 g batches of the compositions examined for this synthesis study.

Jar milling techniques[7] were excluded because the boron component would mechanically plate the inside surface of the jar.

Twin-Shell^{R} solids-solids blending[8] was found to provide uniform, rapid mixing of the powders. Boron-rich inclusions were sometimes observed in the course of the various examinations of the densified reaction pressings, which indicated separation of the powders was possible. However, because of the potential of applying this method to large batch processing, this mix method was selected for this study.

Pre-mixed titanium and boron powders were also processed in a jet or fluid energy mill. Jet milling has attracted considerable attention since it has the distinct advantage of producing fine powders of controlled particle size and distribution while maintaining purity. A schematic representation of the Trost-type jet mill used in this study is shown in Figure 9 . A ...atory hopper feeds the powders to be ground into a stream of compressed

---

(6) Estimate trace < 0.1%.

(7) U.S. Stoneware mill drive, 260 rpm; size 000 mill jars, 13 mm x 13 mm grinding pellets; dry milled 2 hours nominal.

(8) Patterson-Kelley Co., Twin-Shell^{R} yoke solids-solids blender, Model YB-B with YS-1/2 blender shell (working volume = 0.5 quart).

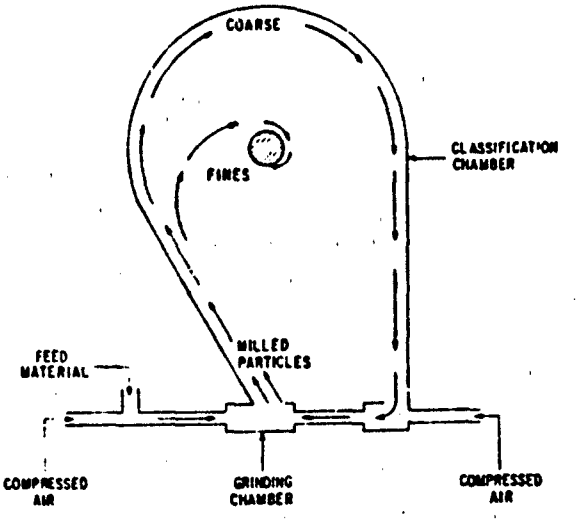

Figure 9. Schematic representation of the essential features of a Trost-type fluid energy mill.

air that is expanded through two diametrically opposed jets. The solid particles are accelerated to very high velocities where particle fracture takes place on collision in a grinding chamber. The rate of grinding is proportional to the jet pressure and the cross-sectional area of the jet opening. After self-attrition of the feed particles, the product particles travel upward into a flat, shallow, circular classifying chamber. Particles with a high surface-to-mass ratio spiral through a central exhaust opening leading to a collector system, whereas those of low ratio continue to travel along the periphery of the classification chamber and are reaccelerated by the second of two jets to collide with new feed material.

The jet-milling method of fine grinding produces a powder with essentially no contamination since there are no moving parts and the liner materials are generally hard ceramics or polyurethane (which can easily be oxidized in a subsequent heat treatment). In addition to the purity considerations, jet milling has also been shown to be preferred over ball milling in terms of particle size and distribution, Figure 10.[9] Note that the jet-milled powder has a narrower particle size distribution (1-6 μm) over the particle size range detected by the Coulter Counter. Furthermore, the average particle size of the jet-milled powder is smaller than that of the ball-milled powder since the entire curve for jet milled powder lies below that for ball-milled powder.

---

(9) C. Greskovich, "Milling" in Ceramic Fabrication Processes, F.F. Wang, Ed., Academic Press, NY, 1976.

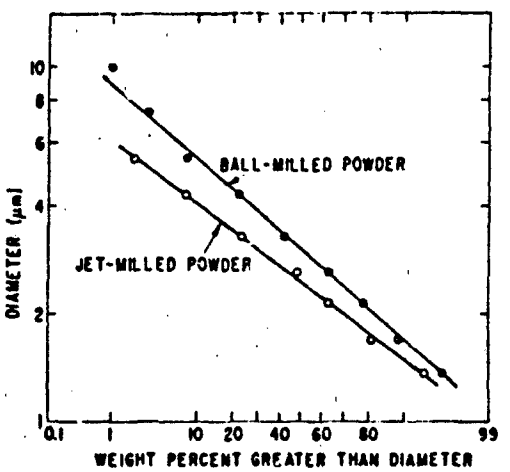

Figure 10. Particle size distribution of ball-milled and jet-milled powders of $(Y, Gd)_3(Fe, Al)_5O_{12}$.

3.4 Reaction Processing

The reaction pressing of the powder mixes was accomplished in an Astro Industries Inc. Model HP20 3560 Hot Pressing System, equipped with a Honeywell Type RI-3 Small Target Radiamatic Pyrometer for heat-radiation detection and process variable input to the Honeywell Digital Control Programmer (DCP) Model 770211. The microprocessor-based DCP provides the means to store and run set point programs.

A graphite die assembly (1.750" ID) with a carbon-carbon filament wound "strongback" contains the compact during processing in a furnace atmosphere of flowing N_2 or argon and with an applied force of 15000 pounds. Temperature of the hot press die assembly was monitored using the L&N Model 8634-C Precision Optical Pyrometer with accuracy at 1035°C $\pm$ 4°C and at 1760°C $\pm$ 8°C. Figures 11 and 12 illustrate time-temperature and time-pressure profiles for the five hot press processes used in this study. Program 1 incorporates two temperature soaks, 15 minutes at 1050°C and 50 minutes at 1760°C; the low temperature soak (1050°C) provided for equilibration of the graphite die mass prior to high temperature (1760°C) sinter densification. Microstructure evaluation indicated that faster ramp-up of the externally controlled temperature would benefit densification during the Ti + 2B reaction,[10] and Program 9 is a result of this recommendation. The remaining programs (M, 5, 6, etc.) were variations attempted in early experiments, and in later work that indicated low temperature (500°C) degassing (Program 1 with de-gas) or high temperature (2000°C) soak (Program 6) would benefit densification.

Table VI presents the details of the reaction processing used to synthesize and densify TiB_2 from the elemental powder mixes characterized for this study program.

---

(10) Personal Communication, Richard E. Tressler to Peter Zavitsanos, Aug. 8, 1984.

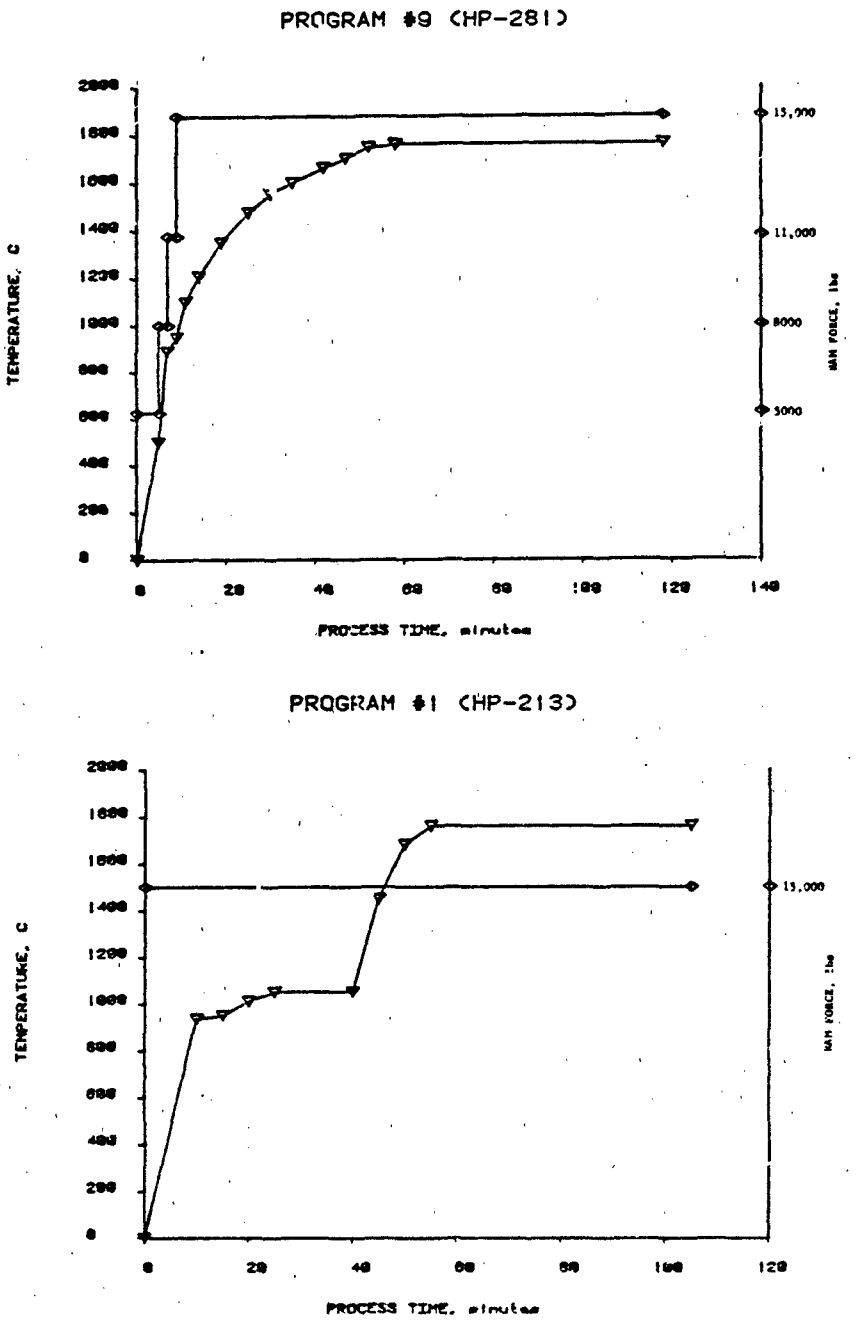

Figure 11. Temperature/pressure-time profiles.

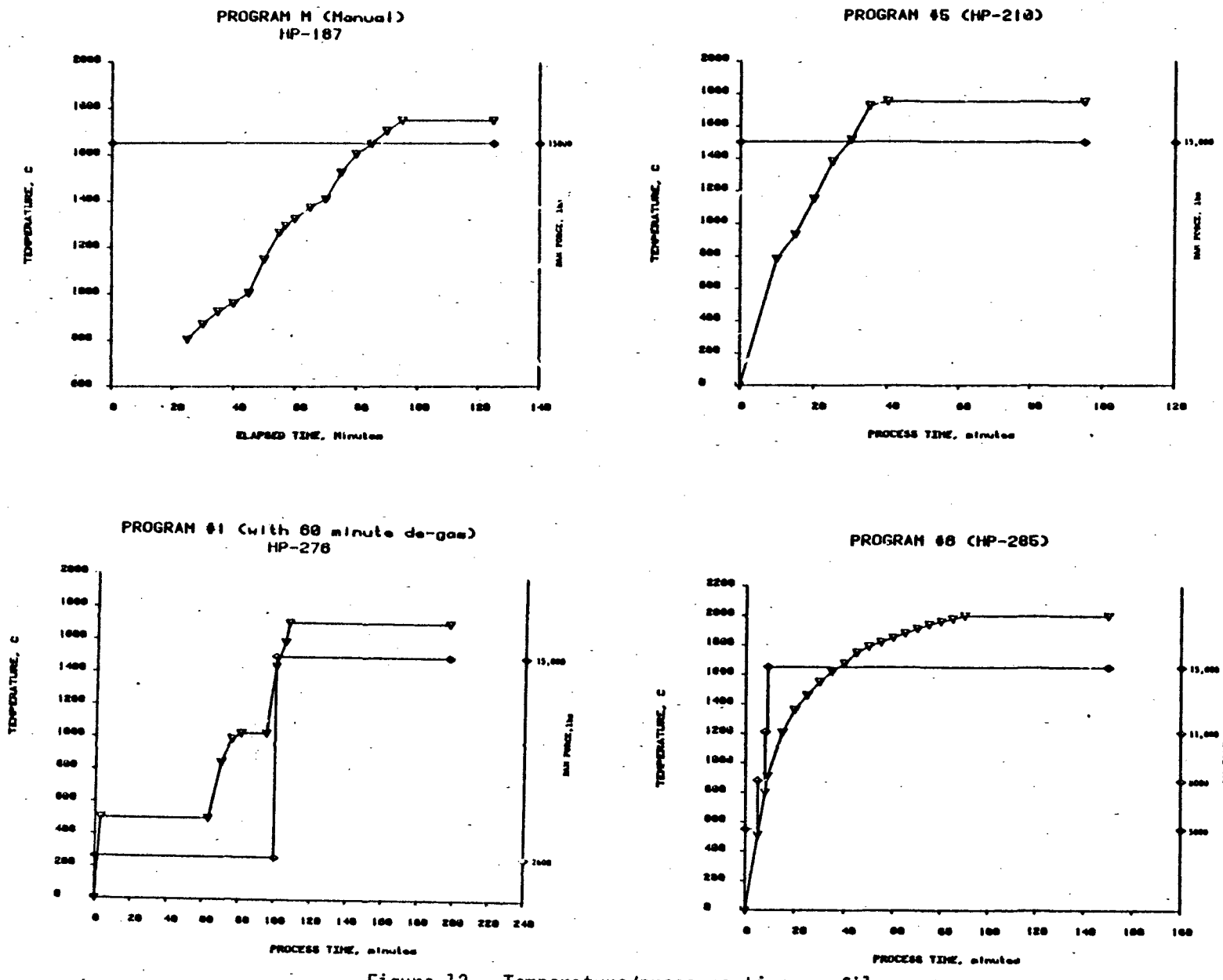

Figure 12. Temperature/pressure-time profiles.

TABLE VI

REACTION PROCESS CONDITIONS FOR TiB_2 SYNTHESIS AND DENSIFICATION

Run #	Powder Mix[1]			Hot Press Set Up[5]					Hot Press Processing[6]									Results
	Titanium[2]	Boron[3]	Stoichiometry[4]	Die System		Release Agent		Pre-Compact (1.a)	Atm	Temp C at Ram Force (10^3 lbs)					Soak: mins @ Temp C		Program	
				L	S	BN	Gr			2.6	5	8	11	15	Low	High		
187	Alfa, -325	Callery, 320 A	Ti + 2B	X		X		5000	N_2	---	---	---	---	20	---	30 @ 1750	H	D = 4.182 96.8%
210	AEE, -325	AEE, -325	Ti + 2B	X		X		5000	N_2	---	---	---	---	20	---	50 @ 1750	S	Broken during removal
211	AEE, -325	Alfa, -60	Ti + 2B	X		X		5000	N_2	---	---	--	---	20	15 @ 1040	20 @ 1760	1	Broken during removal
212	AEE, 1-5 um	Callery, 320 A	Ti + 2B	X		X		5000	N_2	---	---	---	---	20	15 @ 1040	50 @ 1760	1	D = 4.31 95.6%
213	AEE, 1-5 um	AEE, -325	Ti + 2B	X		X		5000	N_2	---	---	---	---	20	15 @ 1050	50 @ 1760	1	D = 4.16 91.9%
214	AEE, -325	AEE, -325	Ti + 2B	X		X		5000	N_2	---	---	---	---	20	15 @ 1050	50 @ 1765	1	D = 4.17 92.1%
215	AEE, -325	Alfa, -60	Ti + 2B	X		X		5000	N_2	---	---	---	---	20	15 @ 1050	50 @ 1760	1	D = 4.020 88.8%
217	AEE, -325	Callery, 320 A	1.049Ti + 2B	X		X		5000	N_2	---	---	---	---	20	---	---	1	Explosion at 820 C
219	AEE, -325	Callery, 320 A	Ti + 2B	X			X	5000	N_2	---	---	---	---	20	15 @ 1060	50 @ 1760	1	Broken during removal
225	Alfa, -325	AEE B_4C, 1-5 um	2Ti + B_4C	X		X		5000	N_2	---	---	---	---	20	15 @ 1060	50 @ 1760	1	Sample not useable
226	AEE, -325	Callery, 320 A	Ti + 2B	X		X		5000	N_2	---	---	---	---	20	15 @ 1040	50 @ 1760	1	D = 4.15 91.7%
227	AEE, -325	Callery, 320 A	Ti + 2.043B	X		X		5000	N_2	---	---	---	---	20	15 @ 1035	50 @ 1760	1	Broken during removal
228	AEE, -325	Callery, 320 A	Ti + 2.043B	X		X		5000	N_2	---	---	---	---	20	15 @ 1025	50 @ 1755	1	D = 3.88 85.7%
229	AEE, -325	Callery, 320 A	Ti + 2.1B	X		X		5000	N_2	---	---	---	---	20	15 @ 1030	50 @ 1760	1	Broken during removal
230	AEE, 1-5 um	Alfa, -60	Ti + 2B	X		X		5000	N_2	---	---	---	---	20	15 @ 1035	50 @ 1760	1	D = 4.31 95.1%
231	Alfa, -325	AEE B_4C, 1-5 um	2Ti + B_4C	X		X		5000	N_2	---	---	---	---	20	15 @ 1035	50 @ 1760	1	D = 2.97 65.6%
265	AEE, -325	Callery, sub-um	Ti + 2B	X		X		5000	Ar	---	---	---	---	20	---	---	1	Explosion at 900 C
269	Alfa, -325	Callery, sub-um	Ti + 2B		X	X		8000	Ar	20	---	---	---	---	---	---	1	Explosion at 935 C
270	Alfa, -325	Callery, sub-um	Ti + 2B		X		X	8000	Ar	20	---	---	---	---	---	---	1	Explosion at 960 C
271	Alfa, -325	Callery, sub-um	Ti + 2.043B		X		X	5000	Ar	---	---	---	---	20	---	---	1	Explosion at 985 C

TABLE VI (CONT'D)

Run #	Powder Mix[1]			Hot Press Set Up[5]					Hot Press Processing[6]									Results
	Titanium[2]	Boron[3]	Stoichiometry[4]	Die System		Release Agent		Pre-Compact (lbs)	Atm	Temp C at Ram Force (10^3 lbs)					Soak: mins @ Temp C		Program	
				L	S	BN	Gr			2.6	5	8	11	15	Low	High		
273	Alfa, -325	Callery, sub-um	Ti + 2B		X		X	8000	N_2	---	---	---	---	20	15 @ 1045	50 @ 1725	1	20 g charge, no explosion
274	Alfa, -325	Callery, sub-um	Ti + 2B		X		X	8000	N_2	---	---	---	---	20	---	---	1	Explosion at 950 C
275	AEE, -325	AEE, -325	Ti + 2B		X		X	8000	N_2	20	---	---	---	1460	15 @ 1025	90 @ 1710	1	D = 4.090 90.2%
276	AEE, -325	AEE, -325	Ti + 2B		X		X	8000	N_2	20	---	---	---	1440	60 @ 500 15 @ 1025	90 @ 1710	1	D = 4.054 89.6%
277	AEE, -325	Callery, sub-um AEE, -325	Ti + 1.81B (AEE) + 0.19B (Cal)		X		X	8000	N_2	20	---	---	---	1200	15 @ 1025	50 @ 1740	1	D = 4.08 90.1%
278	AEE, -325	Callery, sub-um AEE, -325	Ti + 1.62B (AEE) + 0.38B (Cal)		X		X	8000	N_2	20	---	---	---	1250	15 @ 1025	50 @ 1755	1	D = 4.009 88.6%
279	AEE, -325	AEE, -325	Ti + 2B		X		X	8000	N_2	20	---	---	---	1190	---	60 @ 1755	9	D = 4.301 95.0%
280	AEE, -325	AEE, -325	Ti + 2B		X		X	8000	N_2	20	---	---	---	1280	---	60 @ 1750	9	D = 4.291 94.8%
281	AEE, -325	AEE, -325	Ti + 2B		X		X	11000	N_2	---	20	500	890	950	---	60 @ 1750	9	D = 4.284 94.6%
282	AEE, -325	AEE, -325	Ti + 2B		X		X	8000	N_2	---	20	500	---	770	---	60 @ 1760	9	D = 4.282 94.6%
283	AEE, -325	AEE, -325	Ti + 2B		X		X	8000	N_2	---	20	500	825	930	---	60 @ 1755	9	D = 4.295 94.9%
284	AEE, -325	AEE, -325	Ti + 2B		X		X	8000	N_2	---	20	500	---	950	---	60 @ 1750	9	D = 4.270 94.3%
285	AEE, -325	AEE, -325	Ti + 2B		X		X	8000	N_2	---	20	500	800	910	---	60 @ 2000	6	D = 4.038 89.2%
286	AEE, -325	AEE, -325	1.049Ti + 2B		X		X	5000	N_2	---	20	500	---	1050	---	60 @ 1760	9	D = 4.310 95.2%
287	AEE, -325	AEE, -325	1.049Ti + 2B		X		X	5000	N_2	---	20	500	---	930	---	60 @ 1760	9	D = 4.316 95.3%
288	AEE, -325	AEE, -325	1.077Ti + 2B		X		X	5000	N_2	---	20	500	---	930	---	60 @ 1760	9	D = 4.344 96.0%
289	AEE, -325	AEE, -325	1.077Ti + 2B		X		X	5000	N_2	---	20	500	---	970	---	60 @ 1760	9	D = 4.349 96.1%
290	Alfa, -325	AEE, -325	Ti + 2B + 0.017Ni		X		X	5000	N_2	---	20	500	---	980	---	---	9	Explosion at 980 C

TABLE VI (CONT'D)

Run #	Powder Mix[1]			Hot Press Set Up[5]					Hot Press Processing[6]									Results
	Titanium[2]	Boron[3]	Stoichiometry[4]	Die System		Release Agent		Pre-Compact (lbs)	Atm	Temp C at Ram Force (10^3 lbs)					Soak: mins @ Temp C		Program	
				L	S	BN	Gr			2.6	5	8	11	15	Low	High		
291	AEE, -325	AEE, -325	1.077Ti + 2B		X		X	8000	N_2	---	20	500	800	910	---------	60 @ 1760	9	D = 4.314 95.3%
292	AEE, -325	AEE, -325	1.077Ti + 2B		X		X	8000	N_2	---	20	500	825	1030	---------	60 @ 1760	9	D = 4.276 94.5%
293	AEE, -325	AEE, -325	1.077Ti + 2B		X		X	8000	N_2	---	20	500	825	910	---------	60 @ 1760	9	D = 4.301 95.0%
294	AEE, -325	AEE, -325	1.077Ti + 2B		X		X	8000	N_2	---	20	500	810	990	---------	60 @ 1760	9	D = 4.281 94.6%
295	AEE, -325	AEE, -325	1.077Ti + 2B		X		X	8000	N_2	---	20	500	810	950	---------	60 @ 1760	9	D = 4.281 94.6%
296	AEE, -325	AEE, -325	1.077Ti + 2B		X		X	8000	N_2	---	20	500	810	1100	---------	60 @ 1765	9	D = 4.277 94.5%
297	AEE, -325	AEE, -325	1.077Ti + 2B		X		X	8000	N_2	---	20	500	880	1060	---------	60 @ 1760	9	D = 4.300 95.0%
298	AEE, -325	AEE, -325	1.077Ti + 2B		X		X	8000	N_2	---	20	500	700	---	---------	---------	9	Equipment failure
299	AEE, -325	AEE, -325	1.077Ti + 2B		X		X	8000	N_2	---	20	500	---	---	---------	---------	9	Equipment failure
300	AEE, -325	AEE, -325	Ti + 2B 9layers		X		X	none	N_2	---	20	800	---	1050	---------	60 @ 1760	9	Metallography Sample
303	AEE, -325	AEE, -325	Ti + 2B		X		X	none	N_2	---	20	805	885	935	---------	60 @ 1760	9	D = 4.223 95.2%
304	AEE, -325	AEE, -325	Ti + 2B + 0.01 TiB_2		X		X	8000	N_2	---	20	500	845	900	---------	60 @ 1760	9	D = 4.340 96.5%
305	AEE, -325	AEE, -325	Ti + 2B + 0.001 TiB_2		X		X	8000	N_2	---	20	500	830	975	---------	60 @ 1760	9	D = 3.107 68.6% Equipment failure

TABLE VI (CONT'D)

NOTES

(1) Nominally 40 gms loaded into die

(2) HP-291 was first pressing with new AEE -325 Ti powder

(3) Callery 320 Å = 100 micron lamellae

(4) 1.049 Ti + 2B = 5 w/o excess Ti
Ti + 2.043B = 2 w/o excess B
Ti + 2.1B = 5 w/o excess B
Ti + 1.81B + 0.19B = 90.5 w/o AEE B + 9.5 w/o Callery sub-micron B
Ti + 1.62B + 0.38B = 81 w/o AEE B + 19 w/o Callery sub-micron B
1.077 Ti + 2B = 7.5 w/o excess Ti
Ti + 2B + 0.017Ni = 1.4 w/o Ni (Fisher N-40)
Ti + 2B + 0.01 TiB_2 = 1.0 w/o TiB_2 (AEE 1-5 um) added
Ti + 2B + 0.001 TiB_2 = 0.1 w/o TiB_2 (AEE 1 um) added

(5) Die "L" = 4.445 cm ID x 10.2 cm L (1.750" ID x 4.00" L)
Die "S" = 4.445 cm ID x 4.06 cm L (1.750" ID x 1.60" L)
Release Agent, BN = Boron Nitride, Carborundum Series V ($MgSiO_3$ additive)
Release Agent, Gr = 0.015" Grafoil®, Union Carbide Corp

(6) Ram Force of 15×10^3 lbs equivalent to 6706 psi (1.750" ID die)

3.5 Sample Preparation

3.5.1 Machining Techniques

The machining of the TiB_2 reaction pressings to provide various specimens for physical and mechanical property measurements required diamond cutting and grinding equipment. Grinding wheels with 100% concentration of 120 to 180 grit diamond particles proved to be most effective in both slicing and surface dressing of the specimens. Surface cutting speeds in the range of 100 to 120 fpm were utilized with a 0.0005 inch to 0.002 inch downfeed per grinding pass. Table travel was at a low speed and flood coolant was used at all times.

Where possible, a precision vise was used to hold the material during machining, but it was often necessary to wax the TiB_2 to an intermediate clamping block to effectively position the material on the grinding table.

3.5.2 Flexure Bar Preparation

Flexure bars extracted from the reaction pressings were obtained 0.010 inch to 0.015 inch oversize to permit stock removal by precision lap machining. Precision lapping was done on a 15" diameter lap machine[11] with 15 micron B_4C grinding powder in a light oil carrier,[12] after bonding[13] to a lapping fixture equipped with diamond-tipped, micrometer-threaded adjustable stops. After the four long sides are lapped to dimension, the four edges are beveled to remove edge chips and cracks. Beveling was done by hand on an oil-lubricated 1200 grit diamond wheel[14] operated at 125 rpm.

---

(11) Crane Packing Co., Lapmaster 15, with serrated lap plate and conditioning rings.

(12) Lapmaster #3600, 15 μm B_4C, in John Crane 3M oil: 60 g B_4C/1 liter 3M.

(13) Crystal Cement 30C, Universal Shellac and Supply Inc.

(14) 1200 grit ACCU-Finish Wheel, Glendo Corp., with Staidoil diamond lapping oil, Coburn Optical Industries, Inc.

3.5.3 Metallographic Specimen Preparation

Metallography specimens were mounted in a 2-part clear epoxy with mounting filler for edge retention.[15] Grinding and polishing procedures were developed for automatic machine preparation.[16] The procedure uses diamond abrasives and requires four grinding steps (220, 600 grit, 6 and 3 micron) and two polishing steps (3 and 1 micron) with maximum applied force of 300 N (67.4 lbf).

(15) Maraglas 655/555 casting resin, Acme Chemicals and Insulation Co. with -150 mesh soft mounting filler, Buehler Inc.

(16) Abrapol, Struers, Inc.

4.0 EVALUATION OF REACTION PRESSINGS

4.1 Chemical Analyses

Chemical analyses by emission spectroscopy, x-ray diffraction, and electron microprobe examination were applied to selected reaction pressings to assess the results obtained for stoichiometric and off-stoichiometric mixes of selected powder combinations.

4.1.1 Emission Spectroscopy

Table VII summarizes the results of emission spectroscopic analysis for pressings using four types of powders (Alfa -325 Ti, AEE -325 Ti, AEE -325 B and Callery 320A? B). The total metal impurity contents of the reaction pressings: HP187 = 99.4%, HP214 = 99.3%, HP226 = 99.4%, are in good agreement with the purity levels for the elemental powders indicating that contamination control for the numerous steps in the reaction pressing process was effective.

Iron is the most significant impurity, with silicon, aluminum, manganese, and magnesium as secondary contaminants; copper and chromium are present at trace impurity levels.

4.1.2 X-ray Diffraction

Evaluation of x-ray diffraction traces (Ni filtered Cu radiation, λ = 1.54178A) for reaction pressings with stoichiometric composition (HP212, 226) and 7.5% titanium in excess of the stoichiometric composition (HP288, 289) are shown to match the ASTM standard (Card 8-121) for hexagonal TiB_2 (a_o = 3.028A, C_o = 3.228A, D_x = 4.50), Tables VIII and IX. The levels of impurity content and excess Ti are apparently below the limits for detection by x-ray diffractometer methods.

TABLE VII

COMPARISON OF REACTION PRESSING AND ELEMENTAL PURITY FOR THREE PRESSINGS

ELEMENT	WT. PERCENT HP187	HP214	HP226
BORON	M	M	M
TITANIUM	M	M	M
CHROMIUM	0.004	0.02	0.004
MANGANESE	0.12	0.06	0.02
MAGNESIUM	0.02	0.06	0.02
SILICON	0.08	0.12	0.10
IRON	0.2	0.4	0.4
NICKEL	0.02	ND	ND
ALUMINUM	0.12	0.08	0.06
COPPER	0.008	0.008	0.008
TOTAL METAL IMPURITY	0.572	0.748	0.612

	POWDER MIX PURITY		
TITANIUM (PURITY)	ALFA -325 (99%)	AEE -325 (99.7%)	AEE -325 (99.7%)
BORON (PURITY)	CALLERY 320A? (99.9%)	AEE -325 (99.5%)	CALLERY 320A? (99.9%)

TABLE VIII

X-RAY DIFFRACTION ANALYSIS FOR PRESSINGS WITH STOICHIOMETRIC POWDER MIX

HP212*			HP226*			TiB_2 ASTM 8-121		
I	2θ	d,A	I	2θ	d,A	d,A	I	hkl
20	27.50	3.24	30	27.5	3.24	3.22	20	001
50	34.02	2.63	40	34.1	2.63	2.62	60	100
100	44.35	2.04	100	44.39	2.04	2.033	100	101
10	56.95	1.62	10	56.90	1.62	1.613	14	002
15	61.08	1.52	15	61.10	1.52	1.514	20	110
15	68.15	1.38	15	68.20	1.37	1.374	16	102
10	68.40	1.37	10	68.40	1.37	1.370	10	111
	-----		10	72.00	1.31	1.311	8	200
10	78.65	1.22	10	78.70	1.22	1.215	14	201
10	88.40	1.11	10	88.40	1.11	1.104	12	112
	-----			-----		1.020	12	202
10	101.40	0.996	15	101.30	0.997	0.9956	8	103
10	108.50	0.950	10	108.70	0.949	0.9479	10	211

* FROM DIFFRACTOMETER RECORDS - Ni FILTERED Cu RADIATION, λ = 1.54178 A

TABLE IX

X-RAY DIFFRACTION ANALYSIS FOR PRESSINGS WITH EXCESS (7.5%) Ti

X-RAY DIFFRACTION DATA					
HP288*			TiB_2 ASTM 8-121		
I	2θ	d,A	d,A	I	hkl
26	27.59	3.23	3.22	20	001
76	34.22	2.62	2.62	60	100
100	44.49	2.04	2.033	100	101
13	56.95	1.62	1.613	14	002
16	61.20	1.51	1.514	20	110
13	66.08	1.377	1.374	16	102
16	68.17	1.376	1.370	10	111
	----------		1.311	8	200
16	78.75	1.22	1.215	14	201
17	88.48	1.10	1.104	12	112
9	98.50	1.02	1.020	12	202
8	101.20	0.998	0.9956	8	103
12	108.95	0.947	0.9479	10	211

* HP289 ANALYSIS IDENTICAL

AMOUNT OF Ti RETAINED IS BELOW DETECTION LEVEL

4.1.3 Electron Microprobe

The Cameca/Acton MS-64 electron probe x-ray microanalyzer, suitable for x-ray spectrographic analysis down to boron (atomic number 5), was applied to examine compositional gradients in the stoichiometric reaction pressing HP212 (AEE 1-5 μm Ti + Callery 320A?).

The elements detected by x-ray crystal spectrometry were Ti, B, C, Fe, and Si, as shown in the scanning x-ray images, Figure 13. All x-ray images in this figure were obtained in the area identical to the specimen current image. The B K_α and Ti K_α x-ray images have corresponding low concentration areas that are also coincidental with the pore structure shown in the specimen current image. Iron (Fe K_α) concentrations are found only at pore locations, and do not appear to coincide with other impurity sites. The concentration sites for silicon (Si K_α) are coincident with the pore structure; some Si sites are coincident with carbon (C K_α) sites.

This evaluation suggests the impurities are located at pore surfaces and the matrix is TiB_2, as previously established by x-ray diffraction analysis; the script-like inclusions, discussed in Section 4.3, Figure 19, are attributed to TiB. The pore surfaces and adjacent structure are rich in Fe, or Si, or Si + C and compounds containing $Ti_x(B, Fe)_y$, Fe_xB_y, $Ti_x(B,Si)_y$, SiC, and $Ti_x(B,Si,C)_y$ appear possible.

4.2 Physical and Mechanical Properties

Physical and mechanical properties acquisition included bulk density by immersion, three-point and four-point flexure testing, and elastic properties by strain gage and ultrasonic wave velocity measurements.

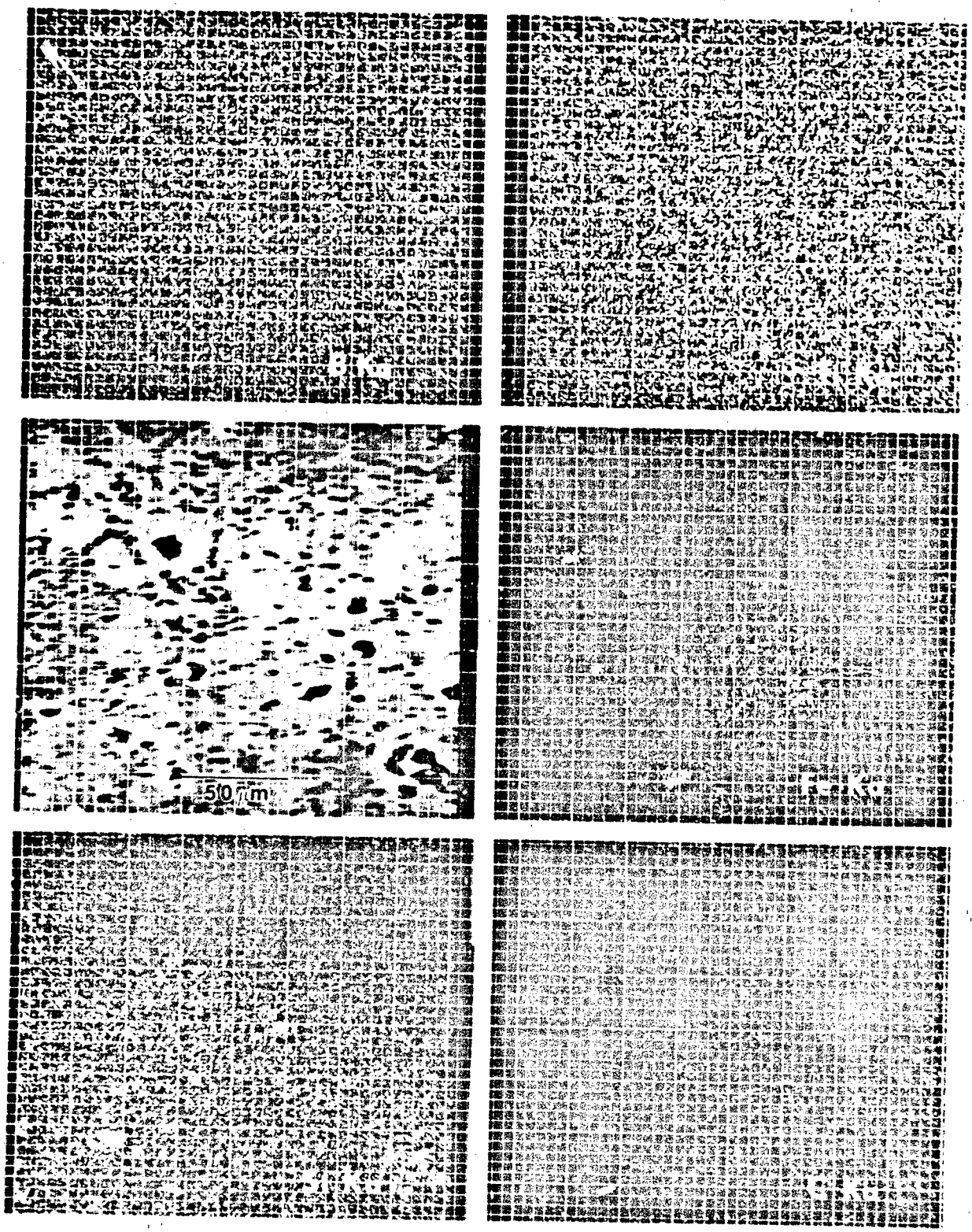

Figure 13. 420X, Electron microprobe examination of HP212 (AEE 1-5 µm Ti + Callery 320A?; 95.6% thecretical density) illustrating concentration gradients of B, Ti, Fe, Si, and C compared to the pore structure.

4.2.1 Immersion Density Measurements

The bulk density of porous bodies requires determination of the total volume of solid plus pores. For samples of regular shapes this can be achieved through measuring sample dimensions and calculating the volume. For irregularly shaped samples, Archimedes principle, which states that a body wholly or partially immersed in a fluid is buoyed up by a force equal to the weight of the fluid displaced, must be applied. For a body of volume V cm^3 immersed in a fluid of density ρ grams per cm^3, the buoyant force F in dynes is given by

$$F = \rho g V$$

where g is the acceleration due to gravity. The bulk density is determined using the following equation:

$$\rho_b = [W_D/(W_D-W_I)]\, \rho_L$$

where W_D is the dry weight of the sample, W_I is the weight of the sample while immersed in the liquid medium, and ρ_L is the density of the liquid at temperature.

The size, shape, distribution, and amount of total porosity can be determined from detailed examination of the microstructure. Alternately, the total porosity can be measured by determining the bulk density ρ_b of a sample (total weight/total volume, including pores) and comparing this with the theoretical or true density ρ_t (total weight/volume of solids). Then

$$f_p = \frac{\rho_t-\rho_b}{\rho_t} = 1 - \frac{\rho_b}{\rho_t}$$

For a crystalline solid such as TiB_2, the density can be calculated from the crystal structure and lattice constant, since the atomic weight for each constituent is known. The weight of each ion per unit cell is given by

(number of sites) (fraction occupied) (atomic weight)/(Avogadro's number). The theoretical density of TiB_2 for this study was calculated as 4.527 gm/cc.

4.2.2 Sonic Modulus

Ultrasonic measurements on TiB_2 plates were made at room temperature and at a frequency of 1.0 MHz by the buffer block method, Table X. In this method, pulses are transmitted from a transmitting transducer to a receiving transducer through a metal plate (the buffer block). The received signal is displayed on an oscilloscope equipped with a calibrated sweep delay. Using the sweep delay, the displayed signal is set to some reference point and the delay reading recorded. The test specimen is then inserted in series with the buffer block so that the signal is further delayed by the transit time through the specimen. Using the sweep delay, the displayed signal is moved to the original reference point and the new delay time reading is recorded. The difference in these two delay time readings is the transit time through the specimen and the wave velocity is the specimen thickness divided by the transit time. The "modulus" is the square of the velocity multiplied by the density.

As the velocity obtained in this measurement is the "plate velocity", the "modulus" thus obtained is higher than the Young's modulus. It is actually the elastic constant C_{11} (assuming an elastic, isotropic material). C_{11} is related to Lame's constant (λ) and the shear modulus (G) by

$$C_{11} = \lambda + 2G$$

whereas Young's modulus, E, is given by

$$E = \frac{G\,(3\lambda + 2G)}{\lambda + G}$$

TABLE X

SONIC MODULUS BY ULTRASONIC WAVE VELOCITY MEASUREMENTS AT 1.0 MHz

SPECIMEN HP NO.	THICKNESS INCH	WAVE VELOCITY KM/S	DENSITY G/CC	TRANSIT TIME μSEC	SONIC MODULUS Msi
281	0.2310	9.878	4.284	0.5940	60.62
282	0.2257	9.911	4.282	0.5784	61.01
283	0.2261	9.8506	4.295	0.5830	60.44
284	0.2248	9.777	4.270	0.5840	59.20
286	0.2270	9.805	4.310	0.5880	60.10
287	0.2260	10.03	4.316	0.5720	63.04
288	0.2250	10.01	4.344	0.5707	63.18
289	0.2247	10.11	4.349	0.5640	64.59

From 4-point flexure tests, $E \approx 60 \times 10^6$ psi and $V \approx 0.1$. From these values of E and V it can be shown that C_{11} is about 2% larger than E. For larger Poisson's ratios the difference becomes larger. For example at V = 0.29, C_{11} is about 30% larger than E. Going in the other direction, C_{11} is about 0.5% larger than E at V = 0.05 and at V = 0 the two are equal.

4.2.3 Flexure Properties

Four-point and three-point flexure tests were conducted using procedures developed in our laboratory for high strength ceramic and composite ceramic materials.[17] Table XI summarizes the flexure property test results.

Four-point flexure tests were conducted using spans of 0.30 and 0.70 inch; four-point was used to obtain a test area of uniform stress so that Young's Modulus and Poisson's ratio could be calculated from strain gage data. The three-point tests were obtained using the larger broken pieces from the four-point tests, which were tested at spans of 0.50 or 0.70 inch, or using a specimen with a small stressed volume (i.e. small dimensions, HP303, 304) at the 0.50 inch span. The relation of three-point to four-point flexure strength has been developed from Weibull Statistics for comparison of the flexure property results.

4.3 Microstructure Examination

Evaluation of microstructure content (grain size, matrix and pore structure, inclusion content), and determination of microhardness and fracture toughness by indentation were obtained to evaluate the results of various powder mixes and reaction pressing processes.

---

(17) Procedures are similar to MIL-STD 1942 (MR), 21 November 1983, "Flexural Strength of High Performance Ceramics at Ambient Temperature."

TABLE XI

FLEXURE AND SONIC MODULUS PROPERTIES SUMMARY

HP	FLEXURE STRENGTH, KSI[1]			MODULUS, MSI	MAXIMUM STRAIN,%	POISSON'S RATIO	SONIC[2] MODULUS, MSI	WEIBULL STATISTICS		
	FOUR POINT SPANS, INCH	THREE POINT SPANS, INCH						WEIBULL MODULUS[3]		CHARACTERISTIC VALUE
	0.3 AND 0.7	0.5	0.7					LEAST SQUARES	MLE	
187	---	82.5[4]	---	---	---	---	---	17.8	16.1	85.0
187	---	46.6[5]	---	---	---	---	---	---	---	---
214	36.1	38.3	---	52.5	0.070	0.083	---	---	---	---
215	32.7	24.1	---	44.6	0.071	0.070	---	---	---	---
226	27.9	34.9	---	52.9	0.042	0.090	---	---	---	---
228	30.3	24.8	---	48.2	0.063	0.083	---	---	---	---
230	48.3	---	---	61.8	0.079	0.069	---	---	---	---
284	43.4	---	47.4	62.5	0.070	0.085	59.2	17.0	29.2	---
288	44.5	---	---	61.4	0.072	0.093	63.2	8.6	11.5	---
289	44.1	---	---	63.3	0.070	0.117	64.6			
303	---	61.8[6]	---	64.2	---	---	---	17.5	15.5	63.6
304	---	57.2[6]	---	65.5	---	---	---	23.3	22.2	58.5

(1) STRESSED VOLUME = 0.250" x 0.050" x SPAN, EXCEPT AS NOTED

(2) SONIC MODULUS MEASURED AT 1.0 MHz, IN-PLANE

(3) MLE = MAXIMUM-LIKELIHOOD ESTIMATOR

(4) STRESSED VOLUME = 0.100" x 0.100" x 0.5"

(5) STRESSED VOLUME = 0.055" x 0.050" x 0.5"

(6) STRESSED VOLUME = 0.115" x 0.087" x 0.5"

4.3.1 Microstructure Content

Microstructure examination and photomicrography was done on a Reichert MeF_2 Universal microscope which is equipped with a twin lamp unit (quartz halogen and xenon burner) and various optical image enhancement devices. Photomicrographs for the intercept method of grain size measurement were obtained using either the Nomarski interference contrast or polarized light attachments.

Photomicrographs of the specimens noted in Table XI, and an SEM examination of microporosity are presented in Figures 14 to 29.

A description of the microstructure content is attempted in Table XII, where the measured grain size ranges from 3.4 μm to 10.1 μm.

4.3.2 Microhardness

Microhardness tests were performed using the Tukon Model MO Microhardness tester equipped for test loads up to 10 kg, as reported in Table XII. The 100 g test load gave the most consistent results; higher loads often produced corner cracking or deformation damage (chipping) at the indent. This damage at the indent was due to densification of the porous TiB_2 under the indent, and required multiple indentations to obtain "readable" indents.

4.3.3 Fracture Toughness

Fracture toughness by indentation (Table XII) was obtained using the same microhardness tester, except that test loads ranged from 1.0 to 6.0 kg. Fracture toughness values were calculated using the methodology suggested by Evans and Charles.[18] Results previously reported[19] have been recalculated

(18) "Fracture Toughness Determinations by Indentation," A.G. Evans and E.A. Charles, J. Am. Cer., Vol. 59, No. 7-8, July-August 1976.

(19) Interim Technical Report for October 1, 1983 to March 30, 1984, Contract No. DAAG46-83-C-0178.

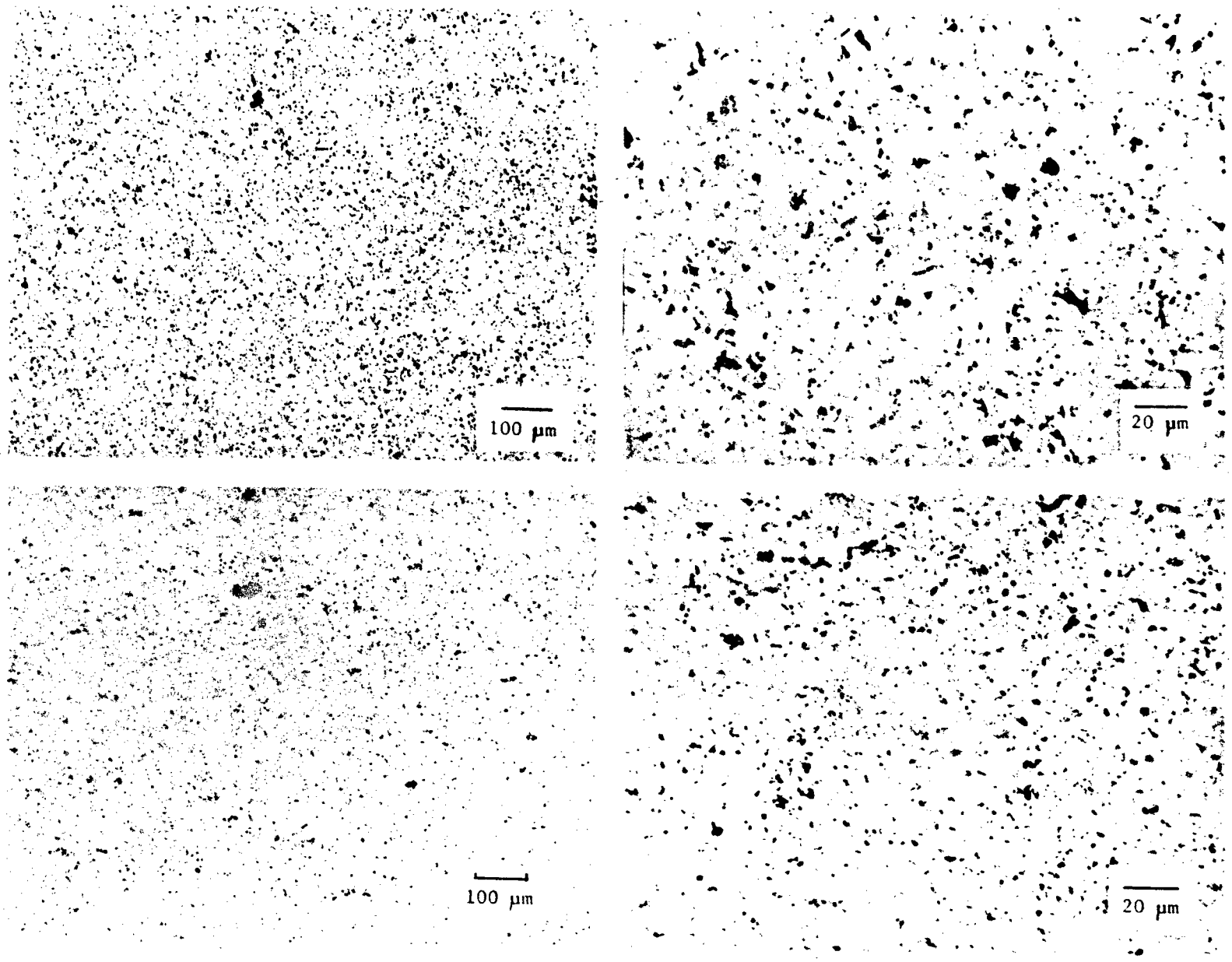

Figure 14. HP 187, Ti (Alfa-325) + 2B (320Å)

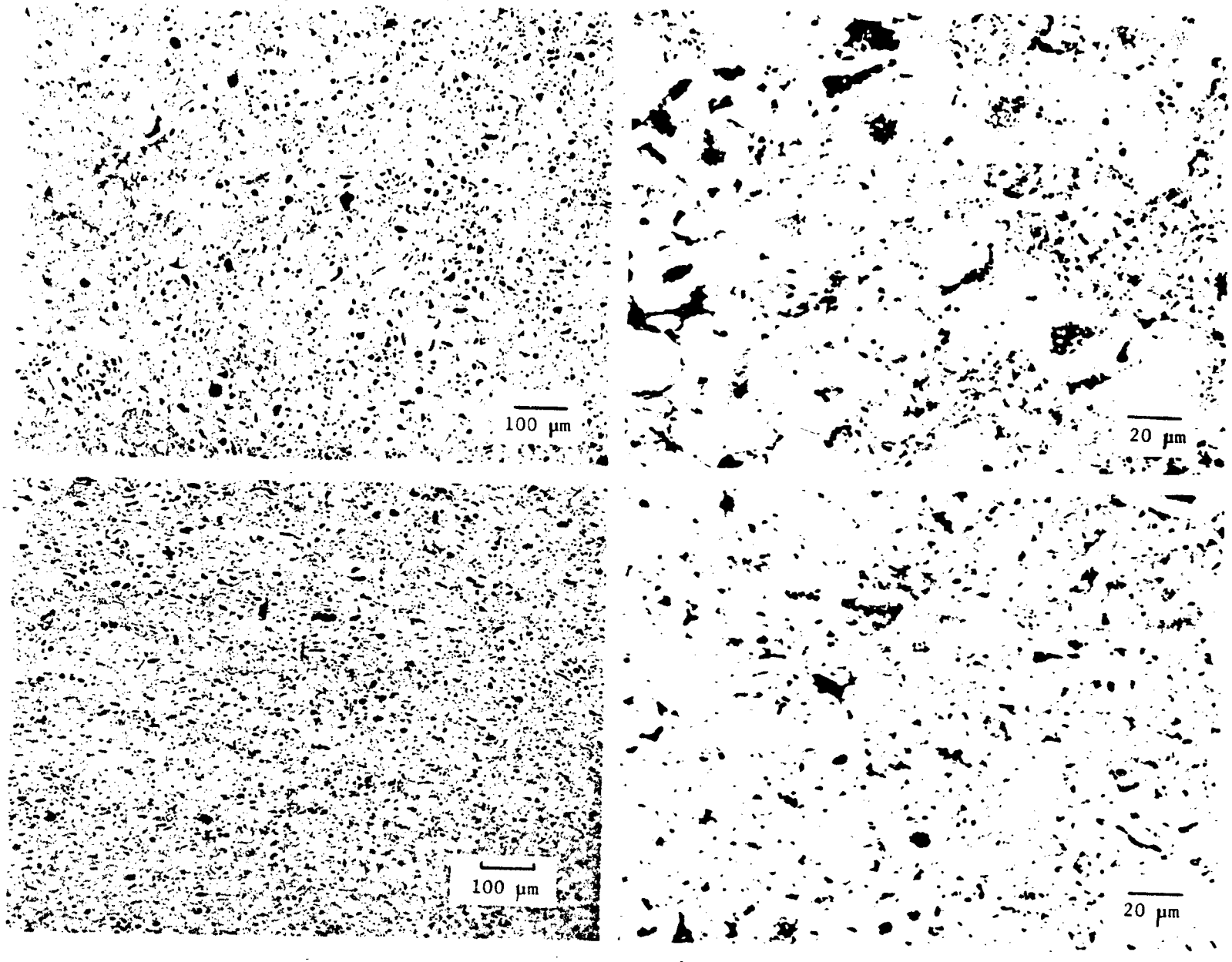

Figure 15 . HP 212, Ti (AEE 1-5 µm) + 2B (320Å)

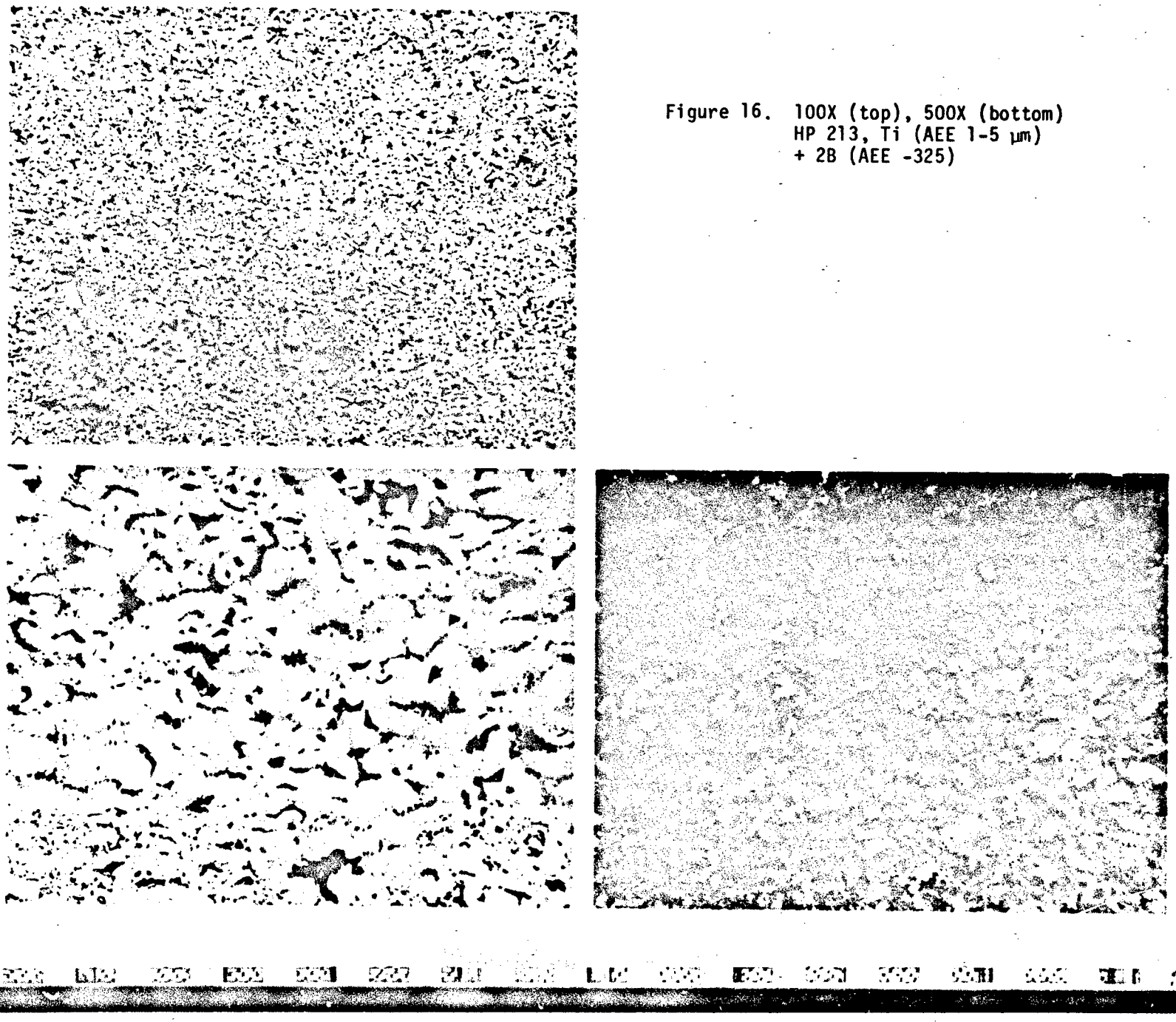

Figure 16. 100X (top), 500X (bottom)
HP 213, Ti (AEE 1-5 μm)
+ 2B (AEE -325)

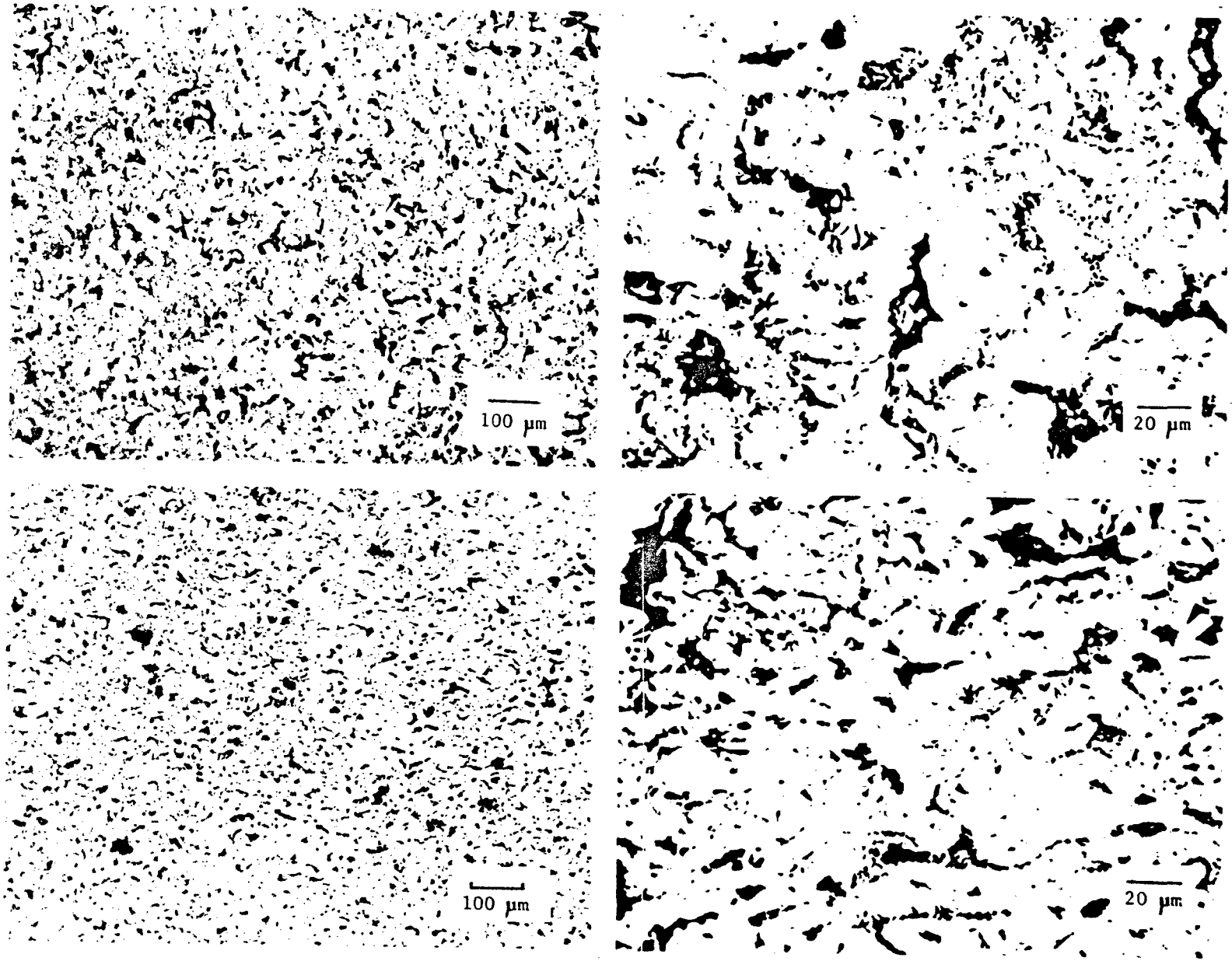

Figure 17. HP 214, Ti (AEE-325) + 2B (AEE-325)

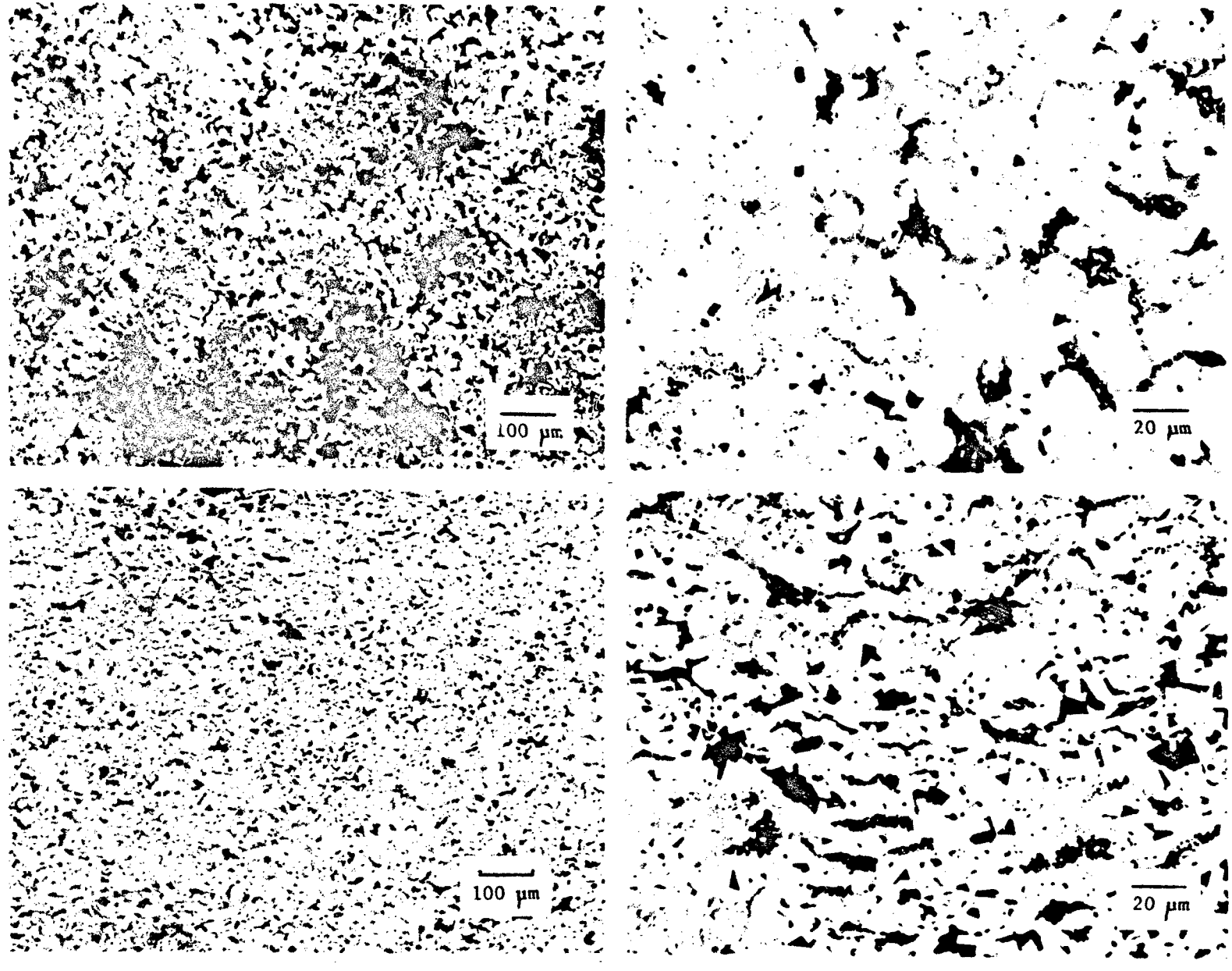

Figure 18. HP 215, Ti (AEE-325) + 2B (Alfa-60)

Figure 19. HP 215, Ti (AEE-325) + 2B (Alfa-60) illustrating microporosity distribution

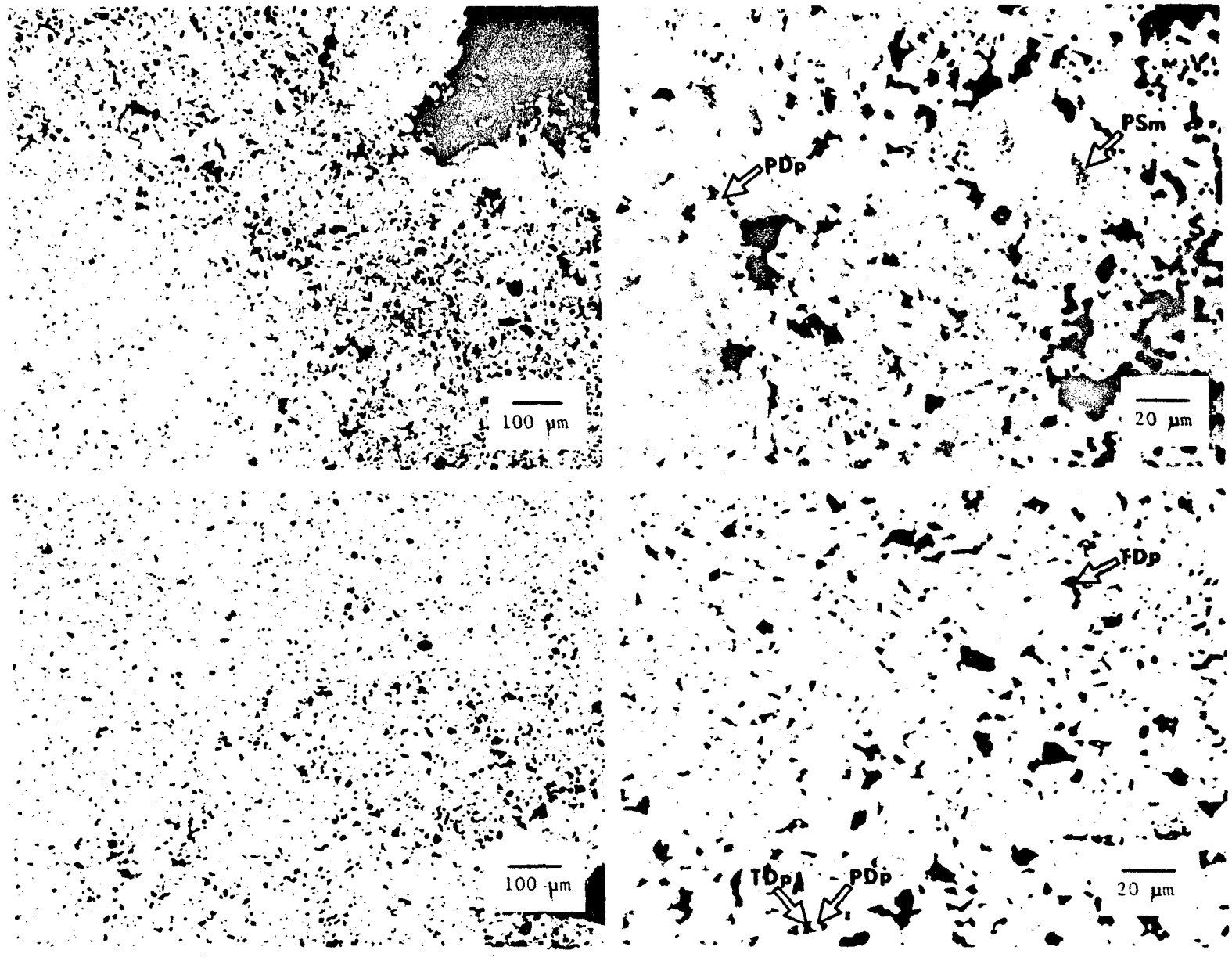

Figure 20. HP 226, Ti (AEE-325) + 2B (320Å); arrows indicate typical phase locations, see Table 3.

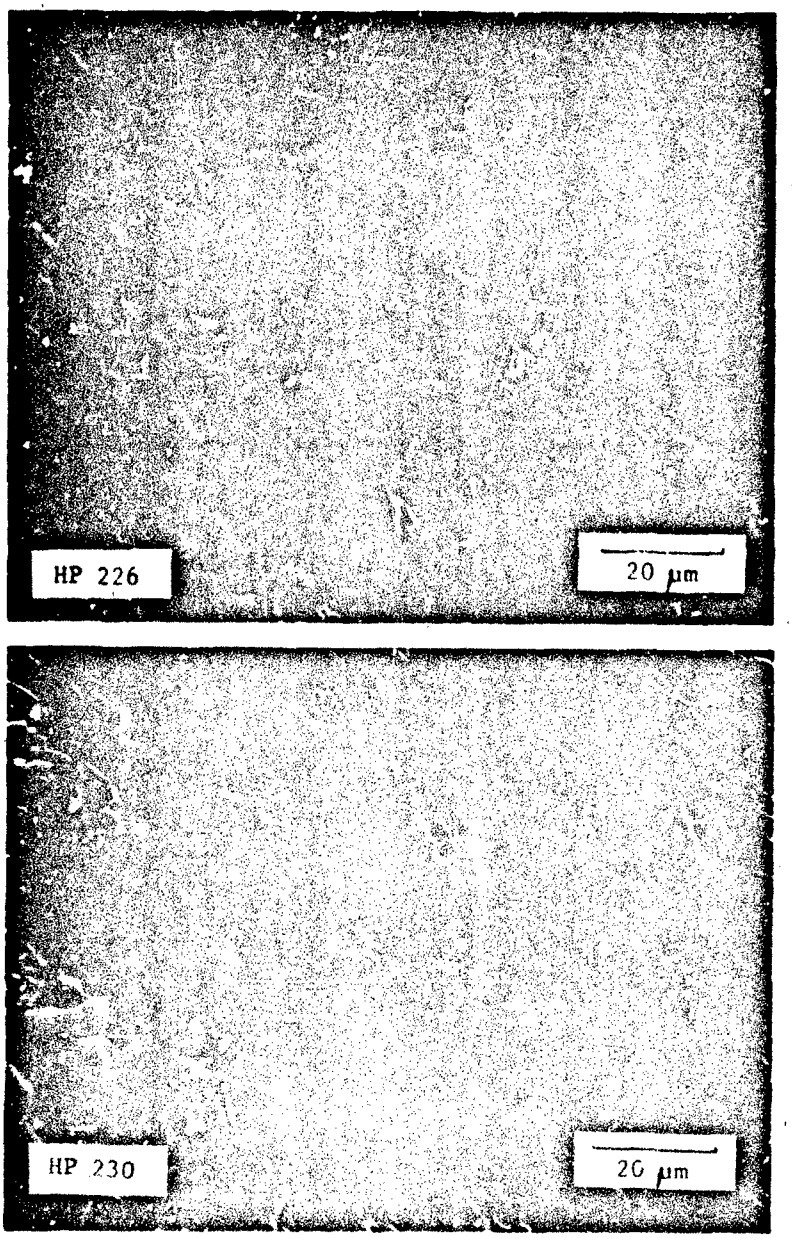

Figure 21. Illustration of variation of observed grain size, preliminary measurements (intercept method are 3.6 µm (top) and 5.9 µm (bottom))

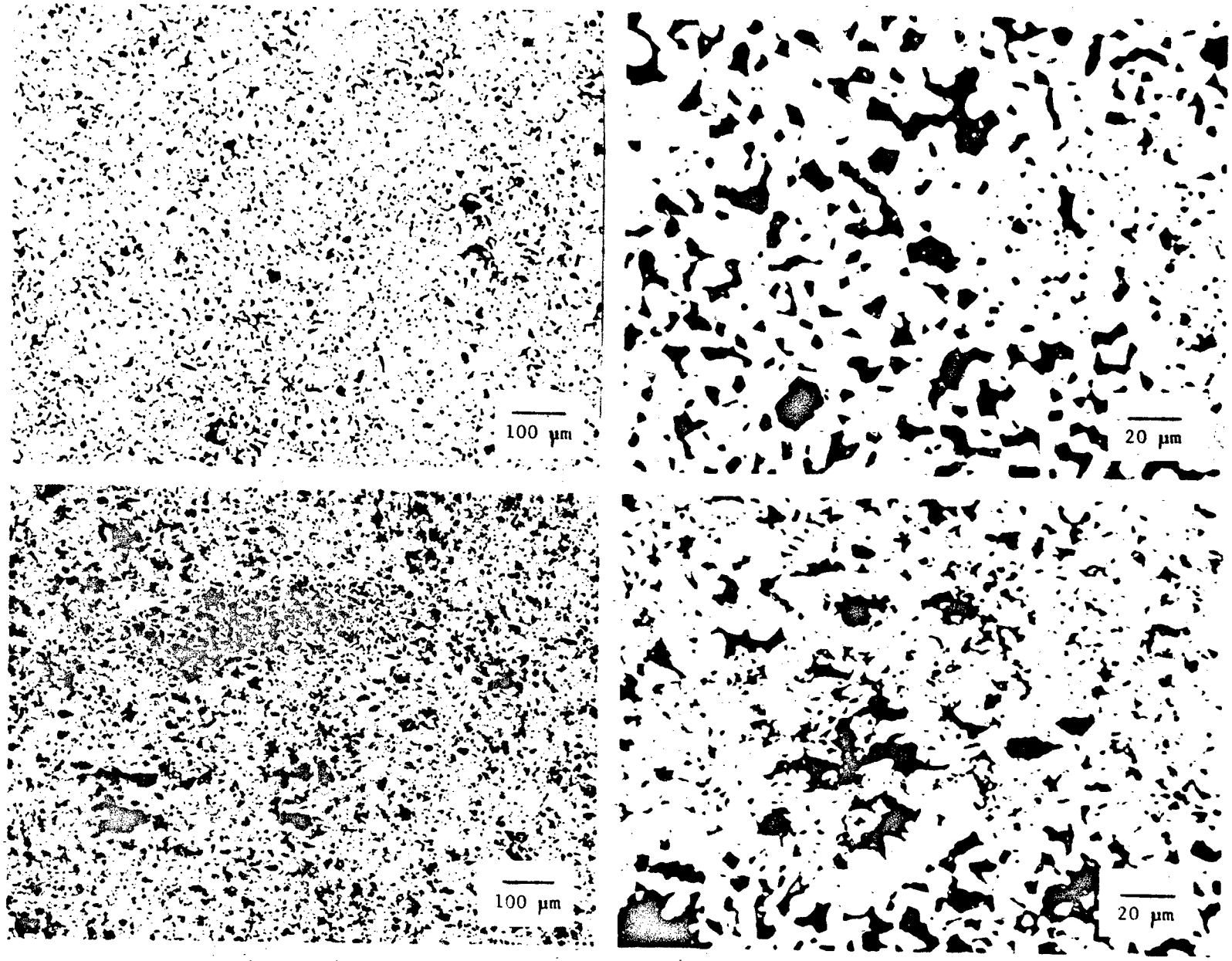

Figure 22. HP 228, Ti (AEE-325) + 2.04 B (320Å)

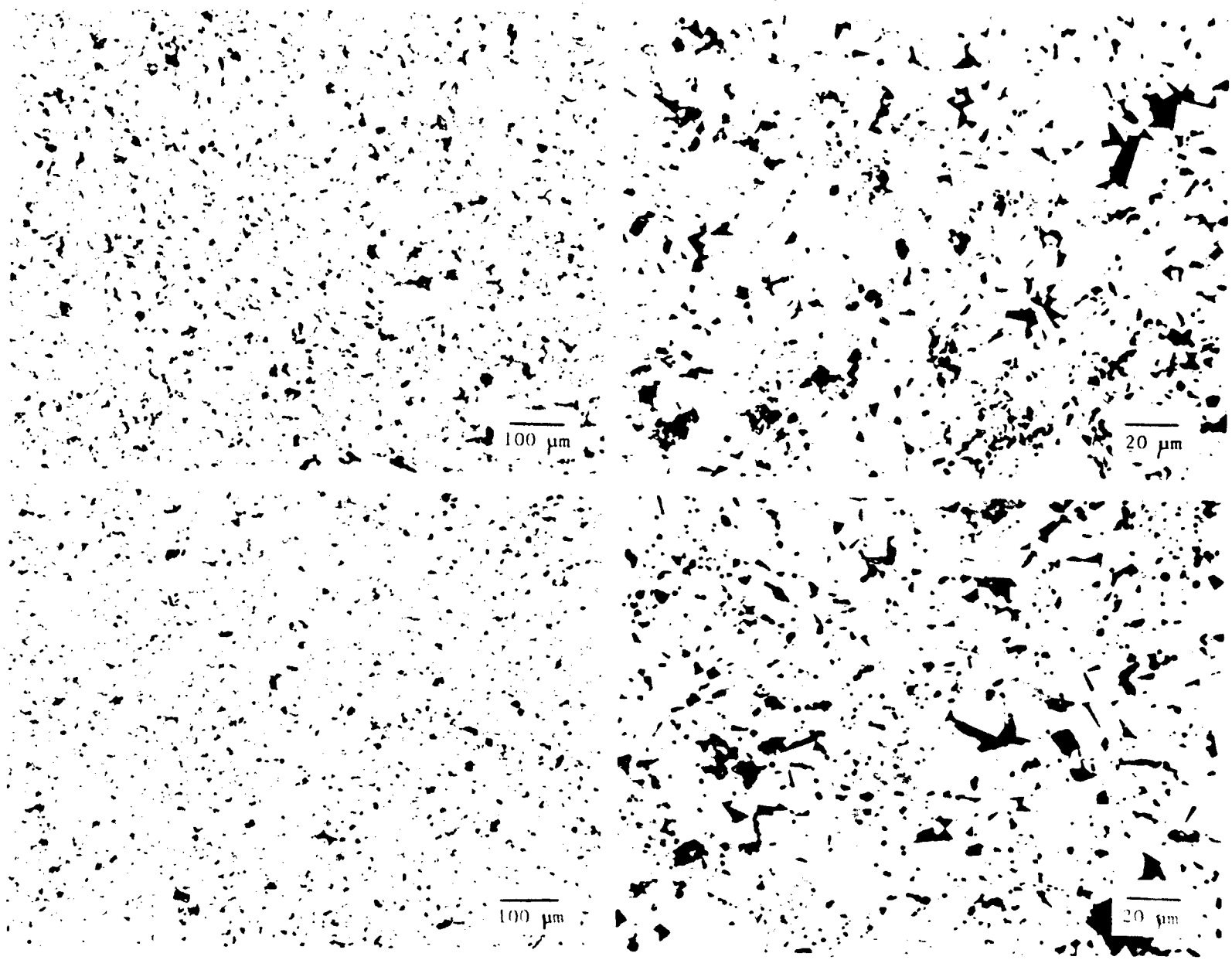

Figure 23. HP 230, Ti (AEE 1-5 µm) + 2B (Alfa-60)

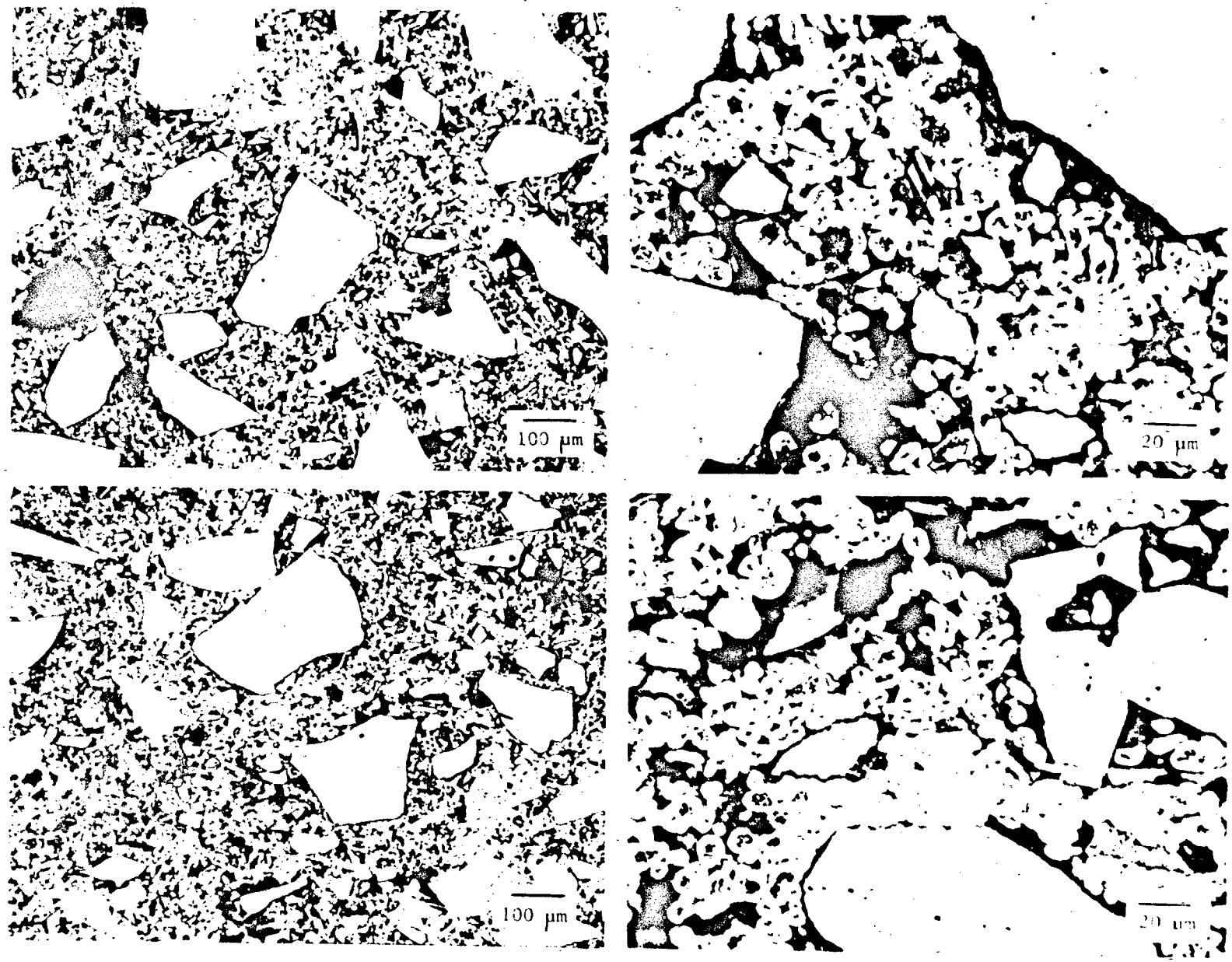

Figure 24. HP 231, 2 Ti (Alfa-325) + B_4C (AEE 1-5 µm)

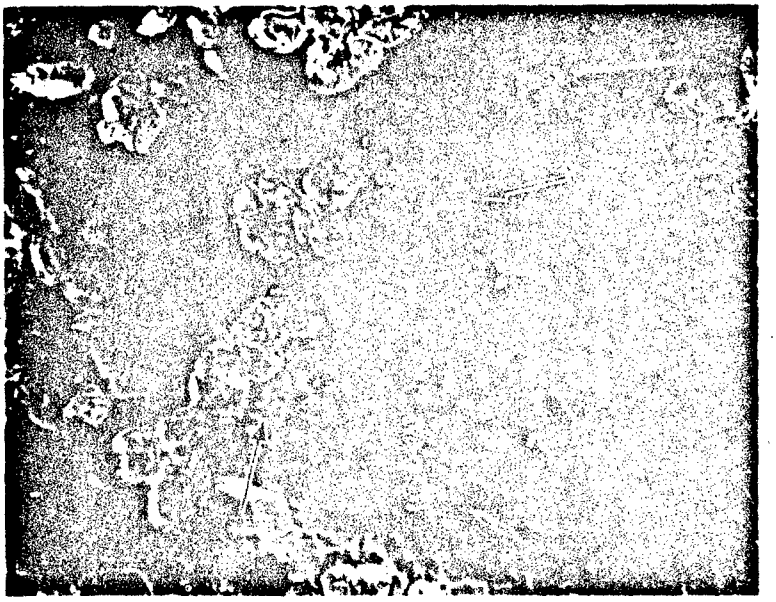

Figure 25. HP 231, 2Ti + B_4C. Detail of interface (arrows) between large particle of thermally-etched B_4C (upper left) and Ti particles (light grey rounded features); 900X, Nomarski interference contrast.

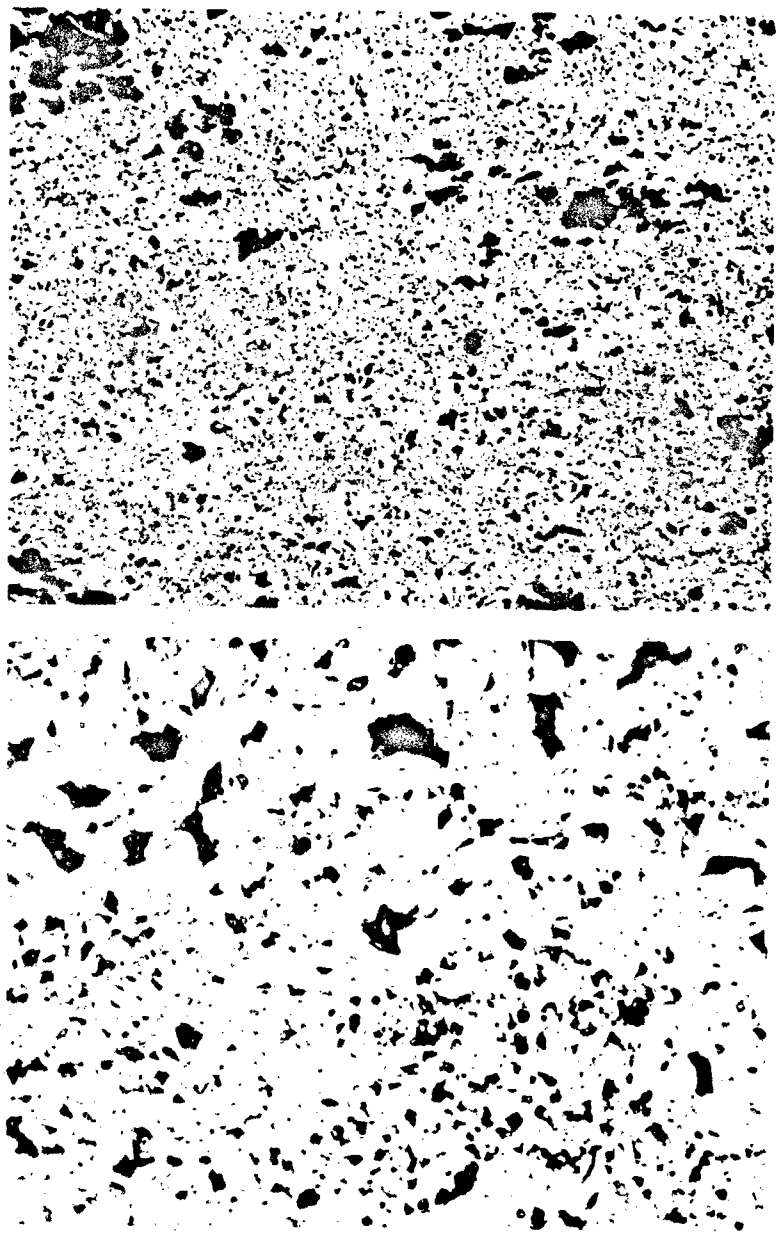

Figure 26. 100X (top), 500X (bottom)
HP 284, Ti (AEE -325)
+ 2B (AEE -325)

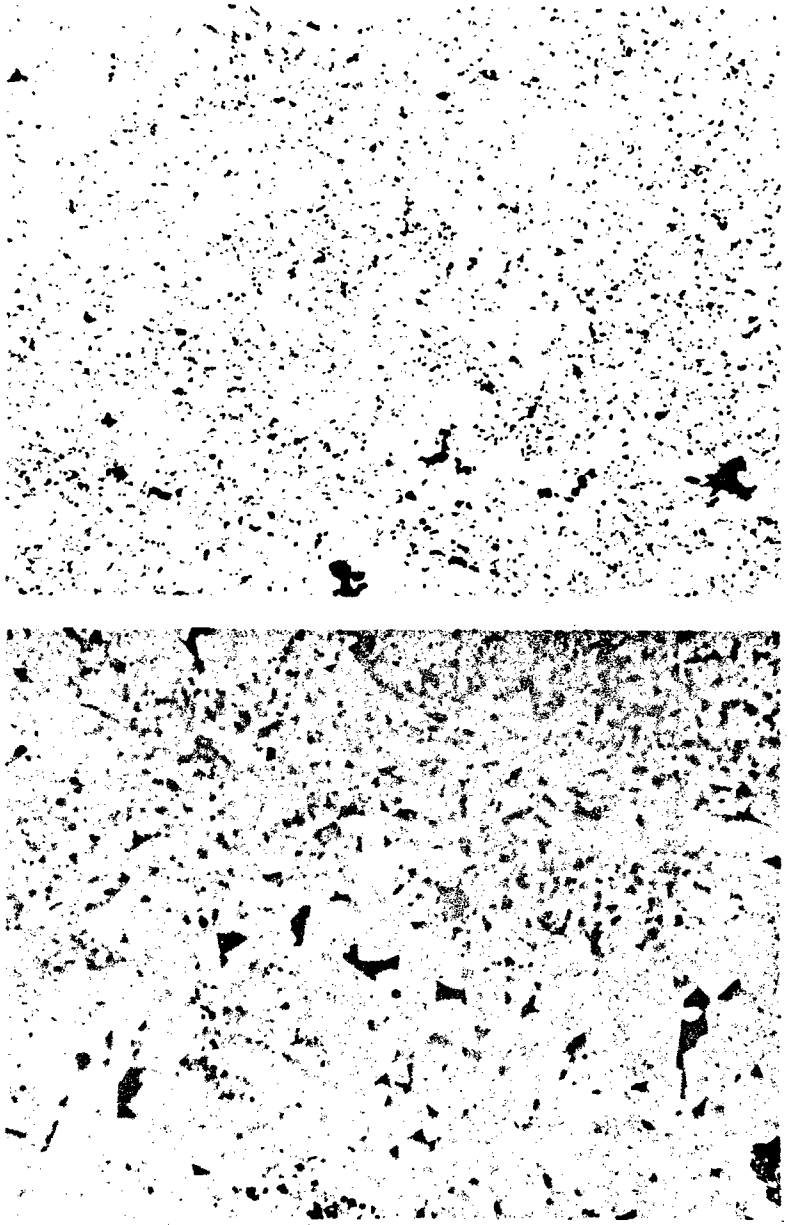

Figure 27. 100X (top), 500X (bottom)
HP 288, 1.077 Ti (AEE -325)
+ 2B (AEE -325)

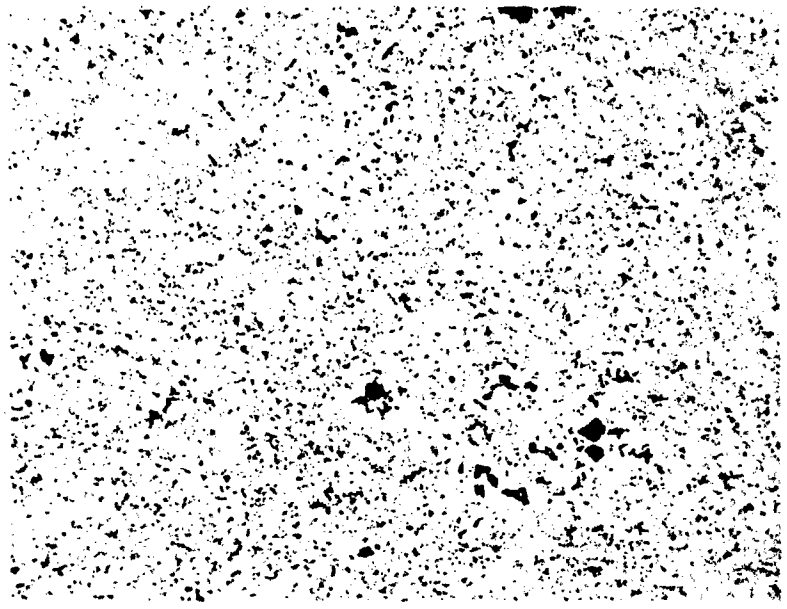

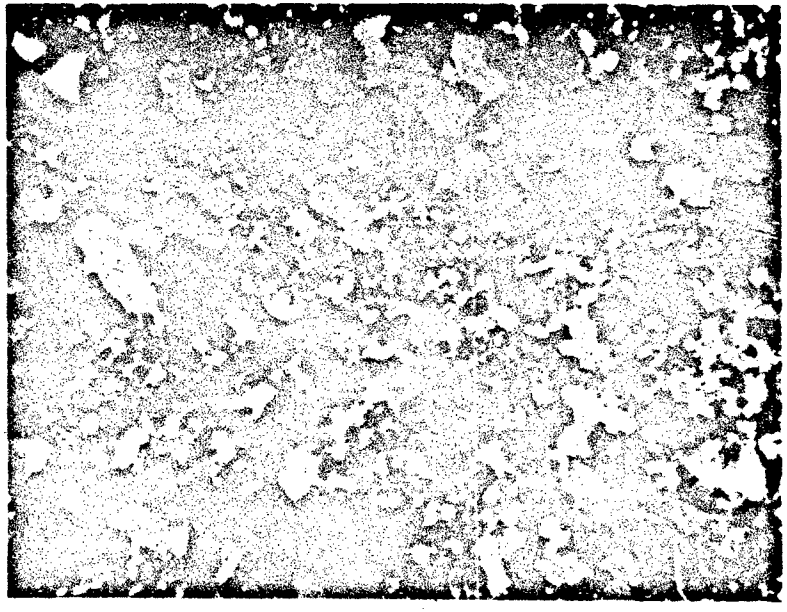

Figure 28. 100X (top), 500X (bottom) HP 289, 1.077 Ti (AEE -325 + 2B (AEE -325)

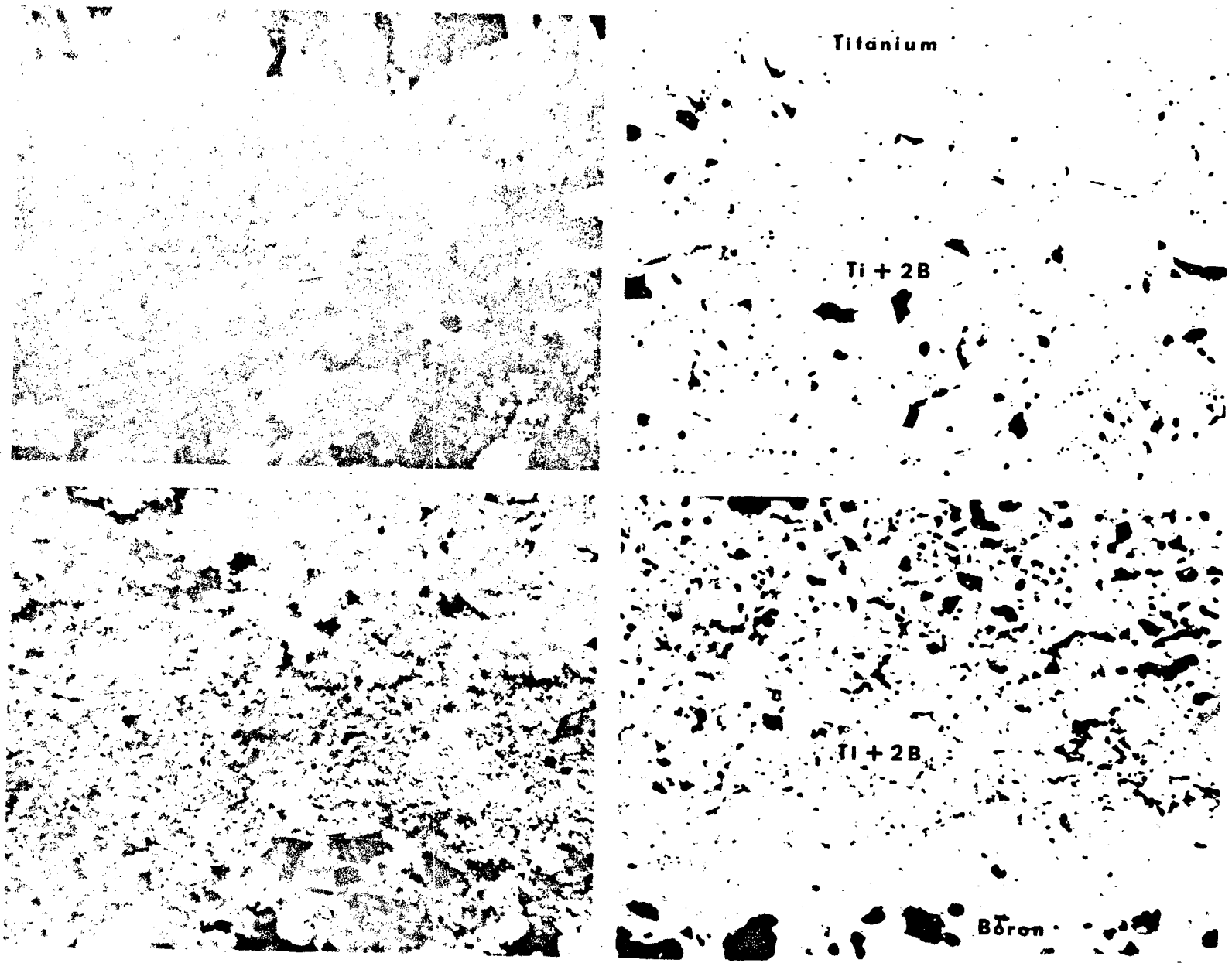

Figure 29. 500X, HP 300, Ti : Ti + 2B : B (Three layer pressing). Top, Ti : Ti + 2B interface, Bottom, Ti + 2B : B interface.

TABLE XII

SUMMARY OF MICROSTRUCTURE CHARACTERIZATION

HP	COMPOSITION[1]	DENSITY[2]		GRAIN[3] SIZE μm	MICRO-[4] HARDNESS, VICKERS, Kg/mm^2	FRACTURE[4] TOUGHNESS, INDENTATION $MN/m^{1.5}$	MICROSTRUCTURE CONTENT SUMMARY			
		IMMERSION g/cm^3	THEORETICAL PERCENT				EQUIAXED[5] GRAIN STRUCTURE	PORE STRUCTURE[6]	MINOR PHASE FORMATION(S)	
									MATRIX	PORE
187	Ti + 2B	4.38	96.8	5.7	2536	5.46	UNIFORM	MICRO.	SCRIPT	DROPLETS
212	Ti + 2B	4.33	95.6	4.1	2703	5.57	UNIFORM	MIXED	--	SCRIPT
213	Ti + 2B	4.16	91.9	7.2	2819	--	BIMODAL	MIXED	--	SCRIPT
214	Ti + 2B	4.17	92.1	5.2	1985	NBI	UNIFORM	MIXED	SCRIPT	SCRIPT; ANGULAR
215	Ti + 2B	4.02	88.8	3.4	2214	NBI	UNIFORM	MIXED	SCRIPT; ANGULAR	SCRIPT
226	Ti + 2B	4.15	91.7	3.6	2753	4.52	UNIFORM	ANGULAR; MICRO.	SCRIPT	DROPLETS
228	Ti + 2.043 B	3.88	85.7	4.7	2736	NBI	UNIFORM	MIXED	--	SCRIPT
230	Ti + 2B	4.31	95.6	5.9	2225	NBI	UNIFORM	ANGULAR; MICRO.	SCRIPT; ANGULAR	SCRIPT; DROPLET
231	2Ti + B_4C	2.97	65.6	---	3239	2.84	MIXTURE	--	--	--
284	Ti + 2B	4.27	94.3	8.4	1946	--	UNIFORM	MACRO. + MICRO.	--	SCRIPT
288	1.077 Ti + 2B	4.34	96.0	9.2	2444	--	BIMODAL	ANGULAR; MICRO.	SCRIPT	SCRIPT; DROPLETS
289	1.077 Ti + 2B	4.35	96.1	10.1	2872	--	BIMODAL	ANGULAR; MICRO.	SCRIPT	SCRIPT; DROPLETS

(1) Ti + 2.043 B = 2 W/O EXCESS B
1.077 Ti + 2B = 7.5 W/O EXCESS Ti

(2) THEORETICAL DENSITY = 4.527 g/cm^3

(3) INTERCEPT METHOD

(4) MINIMUM TEST: 5 INDENTS AT 0.1 kg
MAXIMUM TEST: 15 INDENTS, UP TO 6.0 kg
MICROHARDNESS FOR 213, 284, 288, 289 = MAX. TEST VALUE
TOUGHNESS FOR 231 ON B_4C PARTICLE
NBI = NOT BY INDENTATION

(5) BIMODAL = TWO SIZE GROUPS OF EQUIAXED GRAINS

(6) MIXED PORE STRUCTURE = COMBINATION OF ANGULAR, LENTICULAR, AND ROUNDED MICROPORE SHAPES

using independently measured elastic moduli and 100 g test load hardness data.

The controlled surface flow technique was attempted to obtain an independent measure of fracture toughness.[20] Knoop microhardness indents (average length = 376 μm) were placed on the tension side of 0.250" x 0.050" four-point flexure specimens. No fractures initiated at the site of the indents; fracture stress (flexure strength) of the "worst flaw" specimens was not measureably reduced compared to "unflawed" specimens, indicating other microfeature defects, such as the pore structure, initiated fracture.

(20) "Fracture from Controlled Surface Flows," J.J. Petrovic and M.G. Mendiratta, Fracture Mechanics Applied to Brittle Materials, ASTM STP 678.

5.0 DISCUSSION

5.1 Effects of Microstructure on Properties

The results of the reaction thermochemistry indicate the adiabatic temperature of 3600°K, obtained in the reaction

$$Ti(s) + 2B(s) \rightarrow TiB_2(s) + \Delta H$$

exceeds the melting point of TiB_2, reported as 3063°K (2790°C).[21] Studies of the microstructure of the reaction pressings confirm that a liquid phase is present during the process, and the reaction is in a liquid + TiB_2 phase field. The electron microprobe results indicate that secondary phases (possibly TiB and Ti) and contaminants (Si, Fe, possibly Ti(B,Si), SiC) are rejected from the liquid as the mass cools and are located at pore surfaces and as inclusions in the TiB_2 matrix.

The effect of starting powder purity and grain size on microstructure development and on physical and mechanical properties has been difficult to uncover. Stoichiometric and excess Ti powder mixes react to form TiB_2 with total metal impurities 0.57 to 0.75%. The formation of a liquid during the reaction is a desirable situation and rapid short term densification is predicted. The reaction is homogeneously auto-nucleated by an externally applied thermal gradient to the maximum process hold temperature of 1760°C. This short-term densification occurs during the auto-ignition of the powder mix at low external process temperatures (700°C to 950°C). The externally-applied process temperature continues to increase after the reaction is complete and the heat of reaction is dissipated. During this post-ignition portion of the processing, sintering densification continues and is controlled by kinetics of particle-particle mass transport or transport through secondary

(21) High Temperature Chemistry of the Binary Compounds of Boron, P.W. Gilles, in Borax to Boranes, Advances in Chemistry Series Number 32, Amer. Chem. Soc. 1961.

liquid phases as suggested by the microstructure content. The role of secondary phases and contaminants, present as the metal impurities, may be to provide an interparticle liquid phase for the sintering densification that occurs in the post-reaction portion of the process.

Characterization results (Table XI) indicate mechanical properties (such as flexure strength) are dependent on improvement in final density, Figure 30. The trend of improvement in final density appears to be dependent on improvements in process cycle (continuous external temperature increase versus incremental increases) and changes in powder mixing (jet milling versus solids blending). These process changes have had more effect on properties than powder sources or stoichiometry, with the possible exception of the reaction pressings which used Callery 320Å boron.[22]

The variation in flexural strength with fractional porosity and inverse of grain size is shown in Figures 31 and 32. The relationship between strength and porosity developed from reaction-pressed TiB_2,

$$\ln \sigma = -5.58\ P + \ln 59.9$$

when compared to the Mandorf and Hartwig[23] expression; $\ln \sigma = -3.19\ P + \ln 40.5$, indicates a higher sensitivity (slope) to porosity changes than previously recorded. The variation in flexural strength (Figure 32) appears invalid, since an increase in strength with decreasing grain size is the expected trend, but re-examination of the data indicates the finer grained ($\sim$4 microns) reaction pressings contained considerable porosity, which demonstrates that

(22) HP212, 226, 228, (a) Microhardness exceeded 2700 Kg/mm^2, (b) Fracture toughness measurable by the indentation method. The thin lamellar morphology of the powder suggests a high purity (99.9%) boron source for the Ti + 2B reaction.

(23) "High Temperature Properties of Titanium Diboride", V. Mandorf and J. Hartwig, High Temperature Materials.

Figure 30. EFFECT OF FINAL DENSITY ON FLEXURE STRENGTH

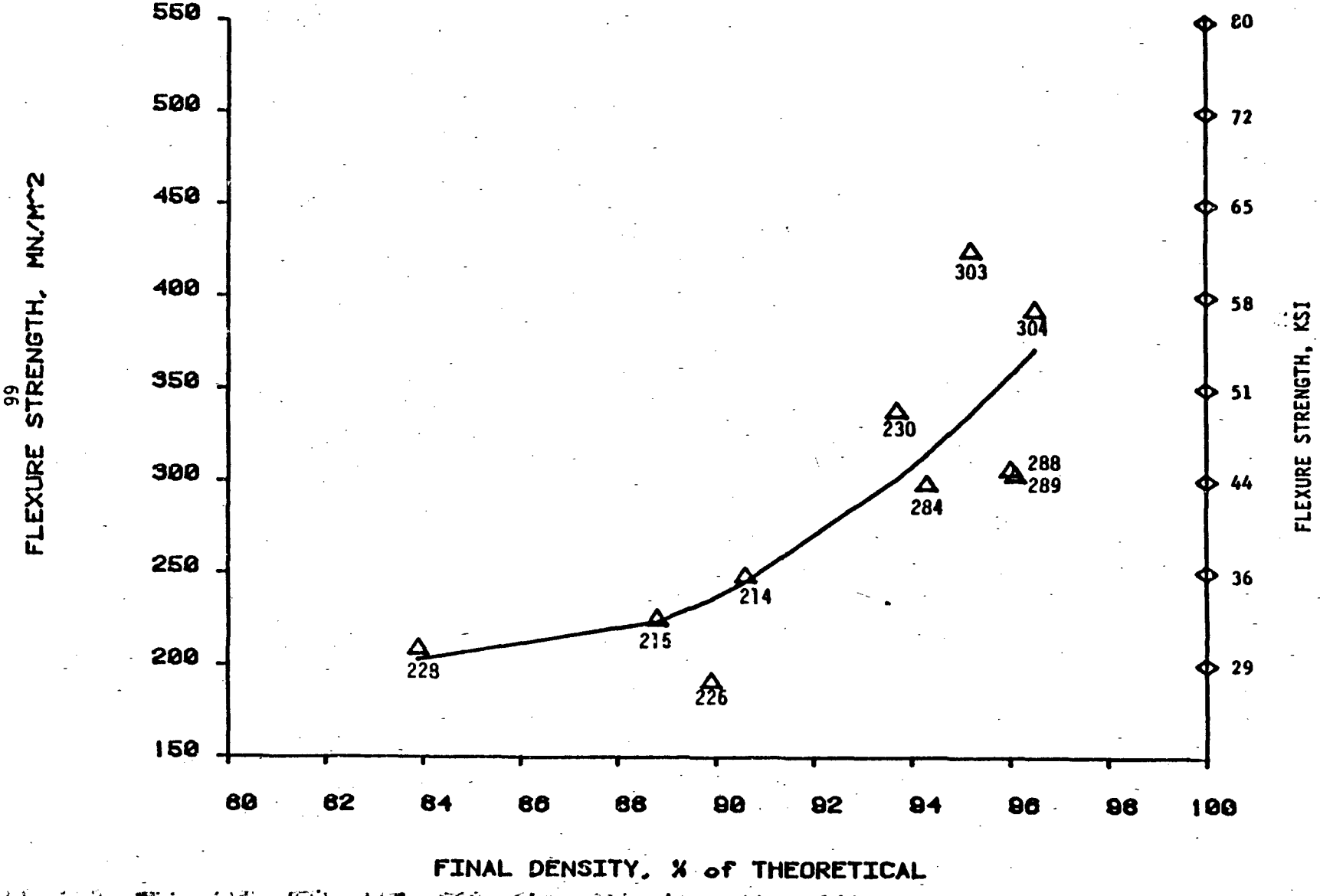

Figure 31. VARIATION OF FLEXURAL STRENGTH WITH POROSITY

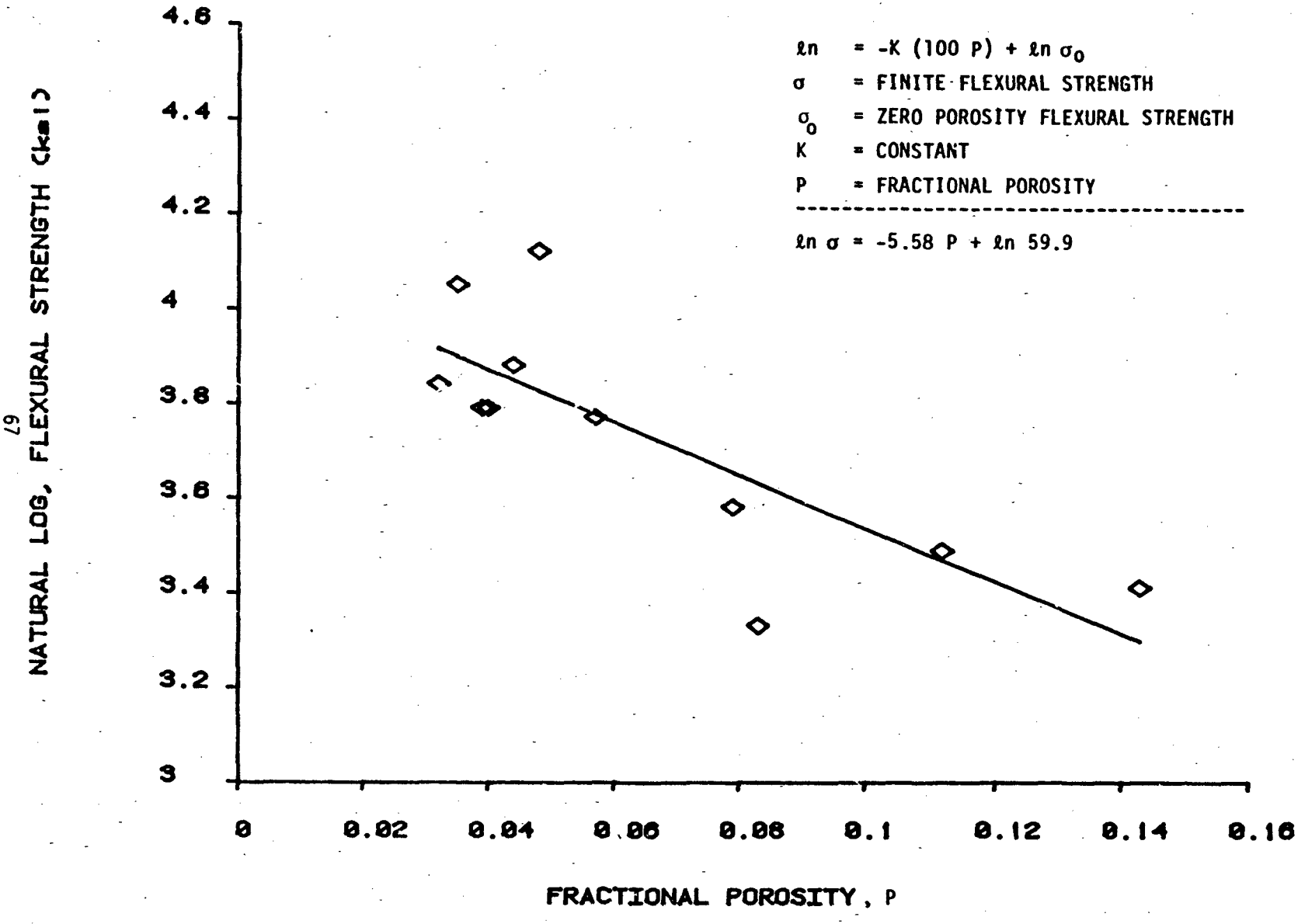

Figure 32. VARIATION OF FLEXURAL STRENGTH WITH GRAIN SIZE

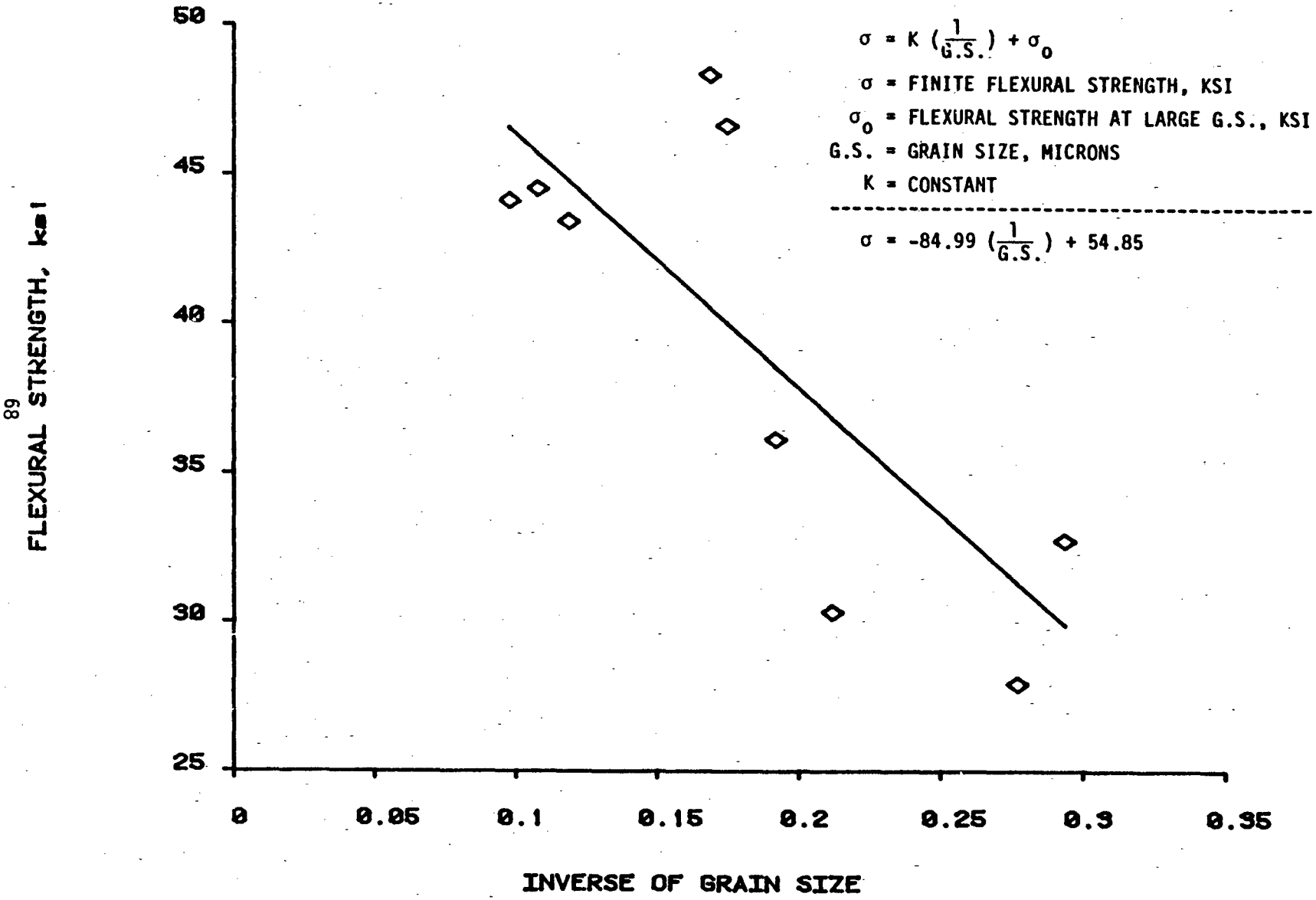

future processing efforts must concentrate primarily on density improvements for enhancement of strength. A critical grain size, ~15 microns (maximum), has been suggested to minimize microcracking due to thermal anisotropy in TiB_2 microstructures.[24,25]

(24) Effect of Microstructure on the Properties of TiB_2 Ceramics, M.K. Ferber, P.F. Becher, C.F. Finch, Communications of the Amer. Cer. Soc., January 1983.

(25) Sintering and Properties of Titanium Diboride Made from Powder Synthesized in a Plasma-Arc Heater, H.R. Baumgartner and R.A. Steiger, J. Amer. Cer. Soc., Vol. 67, No. 3, March 1984.

5.2 Mechanical Property Data Analysis

The relation of 3-point to 4-point flexure strength has been developed from Weibull Statistics.[26] Assuming that fracture is initiated by volume flaws, the cumulative probability of failure (P) is related to stress (σ) and volume (V) by:

$$P = 1 - \exp\left[-\int_V \left(\frac{\sigma}{\sigma_o}\right)^m \cdot dV\right] \quad (1)$$

where m = Weibull modulus and σ_o is a normalizing constant.

For ceramics, m is generally in the range of 5 to 15. The Weibull modulus is related to the scatter, with small scatter for larger "m". Eq. (1) can be integrated to give:

$$P = 1 - \exp\left[-K.V\left(\frac{\sigma_m}{\sigma_o}\right)^m\right] \quad (2)$$

where σ_m = the max. stress (i.e., strength) and K is related to the type of test.

For a 3-point flex test

$$K = \frac{1}{1\ (m+1)^2} \quad (3)$$

For a 4-point flex test

$$K = \frac{m\ (\frac{a}{b}) + 1}{2\ (m+1)^2} \quad (4)$$

where a = inner span
b = outer span.

---

(26) Fracture Statistics in Design and Application, C.A. Johnson, December 1979, GE Report No. 79CRD12.

If one has sufficient data to obtain a good mean value, this can be substituted for σ_m in Eq. (2) and P will be about 0.5. If this is done for both 3 and 4-point data, one obtains

$$\frac{\sigma_3}{\sigma_4} = \left(\frac{K_4 \cdot V_4}{K_3 \cdot V_3} \right)^{1/m} \tag{5}$$

where the subscripts refer to the type of loading.

Table XIII shows the ratio of 3-point to 4-point flexure strength that is predicted by Eq. (5) for the test conditions used and for Weibull moduli of 5 to 20. It is seen that for this range of moduli, the 3-point strengths would be expected to be 15 to 40% higher than the 4-point.

A comparison of the test data is made in Table XIV. Of the four sets of data, that for HP214 shows the lowest scatter and the 3-point mean is about 6% higher. Using normal statistics, this difference is significant (one-sided t-test at 95% confidence level). From Weibull statistics, considering the K·V ratio (Eq. (5)), such a small difference implies a very high Weibull modulus.

For the HP215 specimens the mean for the 4-point tests is 32.73 ksi. Thus the 3-point mean is lower unless one could justify rejection of the 13.18 value, in which case one would conclude that there was probably no difference. A similar situation exists with the HP228 data. If the one low point (8.42 ksi) could be rejected, then the 3-point mean would be lower. Using the Dixon criterion however, this point is not rejectable and hence the two means are about the same.

TABLE XIII

SENSITIVITY OF WEIBULL MODULUS TO FLEXURE STRENGTH RATIO

WEIBULL MODULUS	STRESS RATIO 3-Pt./4-Pt.
5	1.40113103235
6	1.35539313486
7	1.32046924776
8	1.29274190019
9	1.27008609467
10	1.25115980975
11	1.23506815697
12	1.22118855031
13	1.20907283052
14	1.19838922652
15	1.18888629275
16	1.18036961536
17	1.17268626562
18	1.16571412909
19	1.1593544015
20	1.15352619822

IN ADDITION TO THE DIFFERENCE IN TEST MODE (3 vs. 4-Pt.), THE ABOVE RATIO TAKES INTO ACCOUNT THE FACT THAT THE 4-POINT SPECIMENS WERE 40% LARGER IN VOLUME.

TABLE XIV

FLEXURE TEST COMPARISON

LOT NO.	3-POINT SPAN = 0.500		4-POINT SPANS = .300 & .700	
	#	ksi	#	ksi
HP 214	1	38.09	1	34.22
	2	38.76	2	36.28
	4	38.04	3	36.19
			4	37.58
HP 215	1	13.18	1	25.38
	2	35.03	2	43.09
			3	29.86
			4	32.58
HP 226	1	41.61	1	27.13
	2	28.18	2	31.18
			3	18.76
			4	25.33
HP 228	1	27.96	1	30.80
	2	21.73	2	8.42
			3	31.40
			4	28.84

The data on HP226 show considerable scatter and while the 3-point mean is 36% higher than the 4-point mean, the difference is not significant (normal statistics: one-sided t-test at 95% confidence level). From Weibull statistics, a 36% increase, if real, would imply a Weibull modulus of about 6. Calculations of the Weibull modulus from the 4-point data only, by two different methods, gave values of 5 and 7. However, for such a small number of data points these calculations could be corsiderably in error.

In the comparison of HP284 with 288 and 289 and with flexural strength data obtained by AMMRC on HP279, Ti + 2B, groups HP288 and 289 were the same, Table XV. For 4-point flexure the mean strength was 44300 psi (S.D. = 5684). For HP284 the 4-point flexure strength was 43440 psi (S.D. = 2710), Table XVI). This difference is not significant at the 95% confidence level. Of possible importance, 284 appears to have less scatter but again the difference is not significant (95% confidence level). There are too few data points to really be sure.

Weibull moduli were calculated, but the accuracy can be assumed to be poor for so few data points. Results were:

	284	288-289
Least Squares Method	17.2	8.6
MLE Method	29.2	11.5

TABLE XV

4-POINT FLEXURE TESTS AT ROOM TEMPERATURE

(SPANS 0.7" & 0.3")

SPECIMEN #	STRENGTH (psi)	MODULUS (Msi)	MAX. STRAIN (%)	POISSON'S RATIO
HP288-A	39730	61.2	0.065	0.096
-B	49160	60.4	0.081	0.085
-C	44490	62.5	0.071	0.097
MEAN	44460	61.4	0.072	0.093
S.D.	4714	1.06	0.008	0.007
HP289-A	48730	65.1	0.075	0.148
-B	48370	64.9	0.075	0.105
-C	35310	59.9	0.059	0.097
MEAN	44140	63.3	0.070	0.117
S.D.	7648	2.92	0.009	0.027
AVERAGE 288 A,B,C & 289 A,B,C	44298	62.3	0.071	0.105

TABLE XVI

TiB_2 FLEXURE TESTS AT ROOM TEMPERATURE

SPECIMEN #	STRENGTH (psi)	MODULUS (Msi)	MAX. STRAIN (%)	POISSON'S RATIO	NOTES
HP284-1A	39440	62.45	0.063	0.064	
-2A	44750	62.53	0.072	0.101	
-2B	44200	61.95	0.071	0.093	4-POINT
-3A	45370	63.00	0.072	0.082	
					SPANS = 0.7 & 0.3 IN.
MEAN	43440	62.49	0.0695	0.085	
S.D.	2710	0.43	0.0044	0.016	
HP284-1B	45110	---	---	---	
-3B	49670	---	---	---	3-POINT
MEAN	47390	---	---	---	0.7 IN. SPAN
S.D.	3224	---	---	---	

For the HP284, the ratio of 3-point flexure strength to 4-point strength indicates a Weibull modulus of about 30. However, with only two 3-point data points, this could be considerably in error. AMMRC tests on HP279 indicated a Weibull modulus of 19.5 (from 18 tests) and a mean strength of 49000 psi.[27] Based on the AMMRC data, our 3-point specimen would be expected to have a strength of 46630 psi. This is sufficiently close to our mean (47390) that it could be attributed to insufficient data (2-points). However, our 4-point mean is also higher than that predicted from the AMMRC data (43440 vs. 41580) and it is predicted that HP284 flexure strengths would be greater than 49000 if the smaller AMMRC sized specimen were used.

5.3 Increasing Density and Flexure Strength through Powder Processing

Processing of ceramic powders prior to sintering and densification has become well documented in the recent past.[28,29] It is generally agreed upon that certain ceramic powders are more sinterable than others; the degree to which they differ being a function of particle size, size distribution, particle shape, degree of agglomeration, and impurity content. In anisotropic materials such as TiB_2, mechanical properties are usually a function of the microstructure which, in turn, is a function of precursor

(27) "Characterization of SHS TiB_2", Philip Wong, U.S. Army Materials and Mechanics Research Center, April 1985, GE Contract No. DAAG-46-83-C-0178.

(28) "Firing the Proof Test for Ceramic Processing", W.D. Kingery, Ceramic Processing Before Firing, G.Y. Onada, Jr. and L.L. Hench, Eds., Wiley, New York, 1978.

(29) "Concepts in Ultrastructure Processing", L.L. Hench, Ultrastructure Processing of Ceramics, Glasses, and Composites, L.L. Hench and D.R. Ulrich, Eds., Wiley, New York, 1984.

components and method of fabrication.[30] In order to optimize the mechanical properties of TiB_2 fabricated by the self-propagating reaction technique, it will be necessary to carefully characterize the precursor powders in terms of the previously mentioned parameters, and make them more reactive/sinterable.

Considerable effort has been expanded in attempting to delineate mechanisms of sintering in terms of specific equations and diffusion paths. In terms of practical information, the theories have been of great importance in defining what can be done to change the sintering behavior of many materials to promote densification. Regardless of the theory, equation, or mechanism of sintering employed, the rate of densification is inversely proportional to the particle size. This means that the smaller the particle size of the material, the more active the particle will be towards sintering. To put this in perspective, data on various Bager-process alumina powders show that a ten-fold reduction in particle size reduces the sintering temperature by approximately 200°C.[31]

Although it is generally agreed upon that particle size is an important factor, confusion arises because many times small particles are held together in agglomerates. An agglomerate can be defined as a small mass having a network of interconnected pores. They are comprised of primary particles held together by surface forces (soft agglomerates) and/or solid bridges due to sintering, fusion, chemical reaction, or the setting of a binder (hard agglomerates or aggregates). Van der Waal's forces exist between all particles, and predominate for very fine particles under dry conditions. Adsorbed

---

(30) M.K. Ferber, P.F. Becher, and C.B. Finch, "Effect of Microstructure on the Properties of TiB_2 Ceramics," J. Amer. Cer. Soc.

(31) I.B. Cutler, Active Powders," in Ceramic Processing Before Firing, G.Y. Onada, Jr., and L.L. Hench, Eds., Wiley, New York, 1978.

moisture or even moisture condensed between particle contacts are the mechanisms that lead to the commonly observed cohesive powders. All these produce soft agglomerates that can be readily crushed during forming or disrupted by dispersing in a wetting liquid.

Hard agglomerates, on the other hand, resist crushing during ordinary forming and handling. Inappropriate binders often produce hard agglomerates, particularly if the binder has too high a glass transition temperature. Powders prone to hydration can form hard agglomerates in which particles are cemented together by hydrated phases. But by far the most common and deleterious of the hard agglomerates are those native to powders produced by calcination. In this case, particles are connected by strong solid bridges. These can form by ordinary sintering of loose particles at high calcination temperatures or when phase transformations occur by nucleation and growth mechanisms.

It is generally accepted that hard agglomerates retard sintering to theoretical density.[32,33] One of the most obvious effects is the creation of large voids around the aggregate due to poor packing of smaller particles or by the bridging of other aggregates. Such voids, much larger than the surrounding grains, cannot be removed during sintering as there is no driving force for elimination of such oversize porosity. A more subtle effect occurs when closely packed aggregates undergo preferential intra-agglomerate sintering and pull away from neighboring particles leaving large lenticular-shaped voids. This leads to locally inhomogeneous sintering and rapid grain

(32) J.W. Halloran, Agglomerates and Agglomeration in Ceramic Processing," in Ultrastructure Processing of Ceramics, Glasses, and Composites, L.L. Hench and D.R. Ulrich, Eds., Wiley, New York, 1984.

(33) W.H. Rhodes, "Agglomerate and Particle Size Effects on Sintering Yttria-Stabilized Zirconia," J. Amer. Cer. Soc. 64 (1), 19 (1981).

growth in the dense regions where there is no porosity to impede grain boundary migration. Around these isolated aggregates, the inhomogeneous shrinkage creates local microstresses and, in some cases, crack formation.

The remaining factors that effect the sinterability of ceramic powders, namely particle shape, particle size distribution, and impurity content, are essentially secondary to the effects brought about by the particle size and the state of agglomeration. Their role in the sintering process therefore has been the topic of fewer investigations. Regardless, some generalizations can be made. Cutler and Henrichsen[34] found that nonequilibrium (angular) particle shapes of glass sintered more rapidly than equilibrium or spherical particle shapes. This is of significance since grinding produces particles that are angularly shaped. Size distribution is important in practical systems where shrinkage is to be minimized. Mostly large particles and sufficient small particles to fill in the interstices will yield a system of highest green (unfired) density and least amount of shrinkage. However a system of mostly coarse particles will sinter as though it were composed entirely of coarse particles, and the sintering temperature will have to be increased accordingly. Impurities and additives can have dramatic effects on the sintering and densification of ceramic powders. Finding additives that are both grain growth inhibitors and that promote the elimination of porosity is both difficult and time-consuming. In general, though, additives or impurities that form a liquid phase during sintering promote densification while those that do not tend to inhibit densification.

---

(34) I.B. Cutler and R.E. Henrichson, "Effect of Particle Shape on the Kinetics of the Sintering of Glass," J. Amer. Cer. Soc. 51 (10), 604-605 (1968).

The dramatic increase in sintered density and flexure strength of jet-milled titanium and boron powders used to form TiB_2 by self-propagating reaction has been demonstrated. This benefit of powder mixing by jet-milling is seen in comparison of the flexure strength of jet-milled HP303, 426 MN/m^2 (61.8 ksi) and solids-solids blended HP284, 299 MN/m^2 (43.4 ksi). Jet-milling is the preferred method of milling, in this case, since it has been shown to introduce fewer impurities and produce particles with both smaller average particle size and narrower particle size distribution than particles milled by more conventional methods, such as ball milling.[9] The enhanced properties of a jet-milled Ti and B powder mix of stoichiometric 1:2 mole ratio can be attributed to any combination of three factors. First, jet-milling decreases agglomerate size and therefore, overall particle size distribution making the powders more reactive since the sinterability of a powder system is inversely proportional to particle size. Secondly, the self-attrition process produces particles of angular shape that are more reactive than spherical particles. Finally, jet-milling increases the homogeneity of the titanium and boron powder mix which would enable the exothermic reaction to propagate uniformly throughout the body.

Attempts to "seed" the titanium and boron jet-milled powder with/without TiB_2 was slightly less successful. Although the flexure strength of the seeded, jet-milled mix was greater than powders mixed by conventional methods, it was less than that for the unseeded, jet-milled system (57,210 psi vs. 61,770 psi for the unseeded specimen; both being an average of eight flex bar specimens). Further attempts to seed titanium and boron powders will be made, however, by varying both the particle size and the amount of TiB_2 powders added.

5.4 Improvements to Processing

Several areas in the processing scheme of titanium diboride by the self-propagating reaction technique have been identified as sites of potential improvement. Whether oxygen and nitrogen impurities exist in the raw materials and their effect on the reaction are questions that remain unanswered. Oxygen and multi-element neutron activation analysis on the titanium and boron powders both before and after jet milling would determine if this is a problem that needs addressing.

It has been noted[9] that in multi-component systems where large density and particle size differences exist between the powders, jet milling will tend to separate and collect the fine particles of low density and could conceivably alter the initial batch. A way to circumvent this problem would be to first mill the coarser and denser titanium powder, mix with boron, and jet mill the multi-component system.

The green density of a particulate compact, to a large extent, controls the final density of the sintered product. In homogeneous regions in a green compact due to powder particle size or inefficient particle packing result in nonuniform sintering rates which, in turn, create transient stresses. These stresses influence particle rearrangement and may result in the development or enlargement of void space.[35] Maximizing green density, through particle size and distribution control, and efficient die fill, could lead to hot pressed particles free of these strength degrading voids.

---

(35) A.G. Evans, "Considerations of Inhomogeneity Effects in Sintering," J. Amer. Cer. Soc. 65 (10) 497-501 (1982).

5.5 Autoclave Processing

5.5.1 Processing Description

The autoclave, with its 15000 psi capability, represents a method of applying pressure on the titanium/boron powder mix as it transitions from a solid through a liquid phase and back. Figure 33 shows the schematic of the autoclave with a mold in the isolation chamber. Figure 34 is a full-scale drawing of the mold with the powder mixture in place prior to compaction. The vacuum bag (B) keeps the autoclave gas from entering the mold and thereby equalizing the pressure. With the vacuum bag in place the full autoclave pressure is exerted on the moveable plunger of the mold, and will compact the mixture during the reaction phase.

This continually applied force will remain constant until the sample has cooled to room temperature. The autoclave has an internal volume of 27,205 in^3 whereas the compaction volume for a 6" x 6" x 1" plate is only 36 in^3 and in this relationship, when the mold compacts, the overall autoclave volume is increased but such an insignificant percentage that the pressure can be assumed to be constant.

5.5.2 Preliminary Tests

Preliminary autoclave tests were conducted at the 3000 psi level to develop a process data base. During these tests the autoclave was maintained at room temperature and an ignitor wire was used to initiate the reaction. Normal startup difficulties were experienced in obtaining a power path into the autoclave, through the vacuum bag and to the ignitor wire without short circuiting the system. After this difficulty was overcome a successful ignition was conducted at 3000 psi at which time the reaction heat and by-product gas forced the moveable plunger to cock while melting the organic vacuum bag.

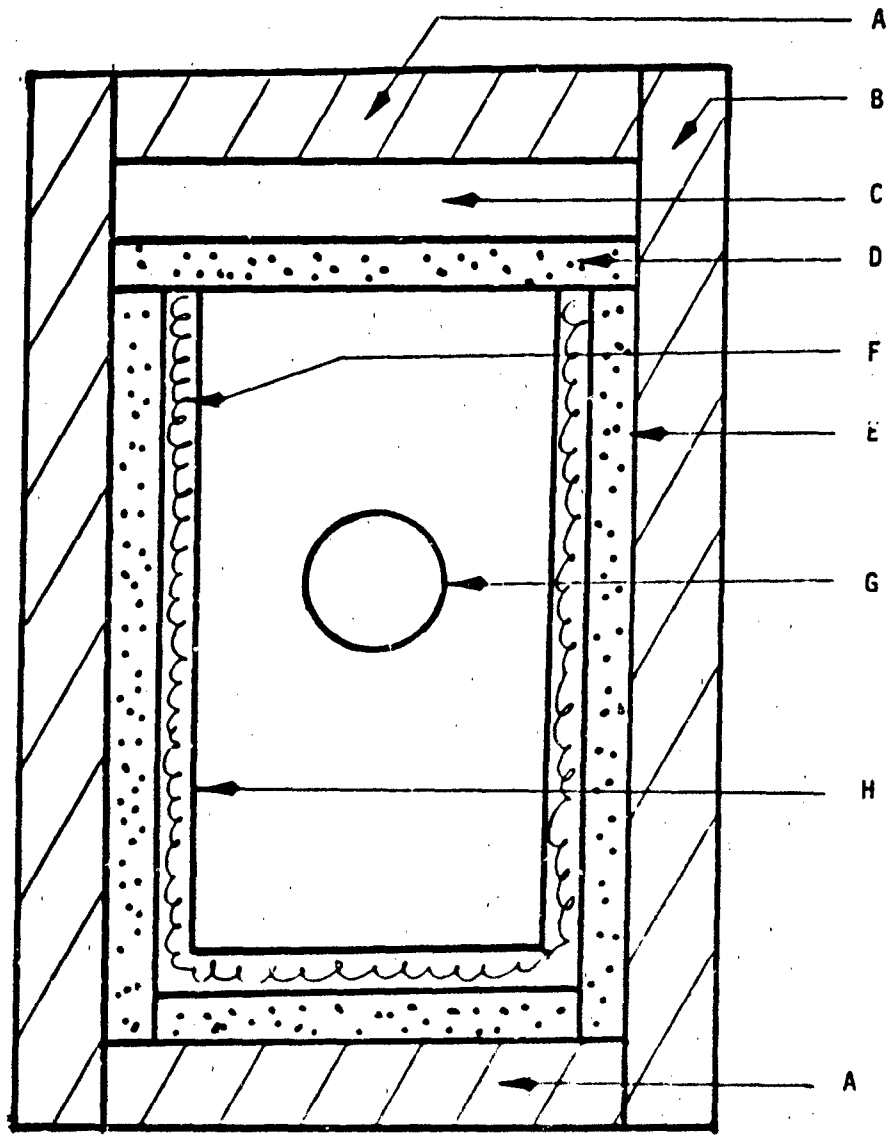

A WATER COOLED HIGH PRESSURE CLOSURE
B WATER COOLED PRESSURE VESSEL
C COOL INSTRUMENTATION SPACE
D INSULATED ISOLATION CHAMBER LID
E ISOLATIOI CHAMBER INSULATION
F ISOLATION CHAMBER HEATERS
G TITANIUM DIBORIDE MOLD (SEE EXPANDED VIEW, FIGURE 31)
H HEATED ISOLATION CHAMBER

Figure 33. High pressure autoclave.

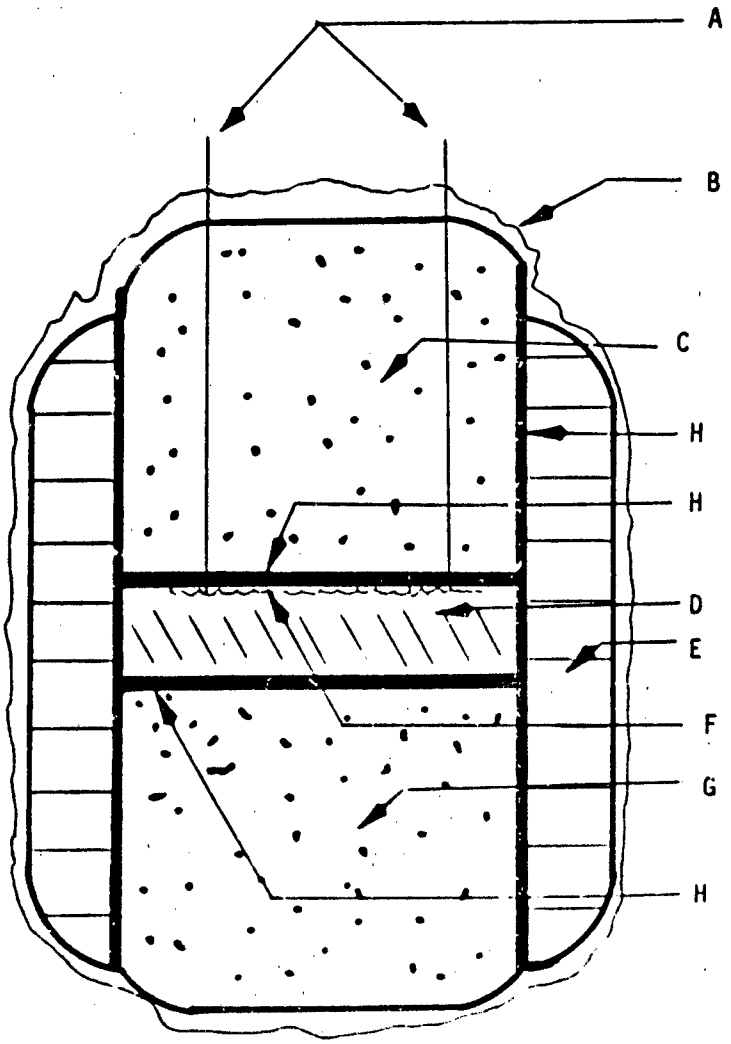

A	LEADS TO IGNITER WIRE
B	VACUUM BAG
C	MOVEABLE MOLD PLUNGER
D	TITANIUM-BORON POWDER MIXTURE
E	MOLD SURROUND
F	IGNITER WIRE
G	MOVEABLE MOLD PLUNGER
H	GRAFOIL LINERS

Figure 34. Autoclave pressure mold - full scale.

It is believed that these problems can be overcome by going up to the 12-15000 psi level and by incorporating a high temperature bag.

5.5.3 Process Scale-Up

The autoclave process appears to offer an excellent method for making the tiles and because of the fairly large autoclave volume one unit could produce a large number of tiles during each run. In a production type of setup, two pressure vessels would be employed and one of the vessels would be brought up to pressure and the tiles made while the second vessel was being loaded with tiles. The high pressure gas from the first process would then be transferred to the second autoclave and the tiles in that autoclave formed while the first autoclave was being emptied and reloaded.

6.0 CONCLUDING REMARKS

1) The heat of the Ti + 2B reaction is sufficient to produce considerable liquid during the process cycle although the relatively fine and uniform grain indicates complete melting is not achieved.

2) The reaction appears to be initiated by the melting of titanium which upon reaction with the boron particle surface produces TiB_2 with the release of chemical energy. This energy is sufficient to liquify the interface and thus provides high diffusion rates; this condition allows continuous transfer of the liquid phase into boron rich regions as exemplified by completion of the reaction.

3) Stoichiometric powder mixes, when prepared by jet-milling, produce a significant increase in flexure strength properties in the reaction pressing.

4) Powder mixes with excess Ti (5.0 and 7.5 weight percent) produce TiB_2 pressings very similar in properties to stoichiometric mixes, when powder preparation was solids-solids blending. However, powder mixes with excess B (2.0 weight percent) were low density (less than 85%) and lower strength than stoichiometric powder mixes.

5) Flexure strength is maximized when density is maximized. Improvements in strength are more sentitive to processing methods than to input powder size and chemistry, although the powder characteristics are seen to be important.

6) It appears that the next phase of this study should proceed in the following direction:

   a) Provide more rigorous powder characterization.

   b) Achieve optimum powder mixing prior to reaction.

   c) Proceed with process scale-up in order to achieve sizes which can be meaningfully tested.

DISTRIBUTION LIST

No. of Copies	To
	Office of the Under Secretary of Defense for Research and Engineering, The Pentagon, Washington, DC 20310
1	ATTN: Mr. J. Persh
1	Dr. G. Gamota
2	Commander, Defense Technical Information Center, Cameron Station, Building 5, 5010 Duke Street, Alexandria, VA 22314
1	National Technical Information Service, 5285 Port Royal Road, Springfield, VA 22161
	Director, Defense Advanced Research Projects Agency, 1400 Wilson Boulevard, Arlington, VA 22209
1	ATTN: Dr. E. C. Levinthal
1	Dr. S. Wax
1	Dr. W. Wilcox
1	Technical Library
	Battelle Columbus Laboratories, 505 King Avenue, Columbus, OH 43201
1	ATTN: Mr. V. D. Linse
	Commander, Army Research Office, P.O. Box 12211, Research Triangle Park, NC 27709
1	ATTN: Information Processing Office
1	Dr. G. Mayer
1	Dr. J. Hurt
	Commander, U.S. Army Materiel Command (AMC), 5001 Eisenhower Avenue, Alexandria, VA 22333
1	ATTN: AMCDM-ST
1	AMCLD
	Commander, Harry Diamond Laboratories, 2800 Powder Mill Road, Adelphi, MD 20783
1	ATTN: Technical Information Office
	Commander, U.S. Army Missile Command, Redstone Arsenal, AL 35898
1	ATTN: Technical Library
	Commander, U.S. Army Armament, Munitions and Chemical Command Dover, NJ 07801
1	ATTN: Technical Library

No. of Copies	To
	Commander, U.S. Army Armament, Munitions and Chemical Command, Rock Island, IL 61299
1	ATTN: AMSAR-LEP-L
	Commander, U.S. Army Armament, Munitions and Chemical Command, Aberdeen Proving Ground, MD 21005
1	ATTN: AMDAR-ACW
1	AMDAR-TSB-S
1	AMDAR-BLP/Dr. J. R. Ward
	Commander, U.S. Army Foreign Science and Technology Center, 220 7th Street, N.E., Charlottesville, VA 22901
1	ATTN: Military Tech, Mr. W. Marley
1	Mr. J Crider
	Chief of Naval Research, Arlington, VA 22217
1	ATTN: Code 471
1	Dr. A. Diness
1	Dr. R. Pohanka
	Naval Research Laboratory, Washington, DC 20375
1	ATTN: Mr. G. Richardson
1	Dr. W. J. McDonough
	Commander, U.S. Air Force of Scientific Research, Building 410, Bolling Air Force Base, Washington, DC 20332
1	ATTN: CPT S. Waks
	Commander, U.S. Air Force Wright Aeronautical Laboratories, Wright-Patterson Air Force Base, OH 45433
1	ATTN: AFWAL/MLLM, Mr. K. S. Mazdiyasni
	National Aeronautics and Space Administration, Washington, DC 20546
1	ATTN: C. Bersch
	National Aeronautics and Space Administration, Lewis Research Center, 21000 Brookpark Road, Cleveland, OH 44135
1	ATTN: Dr. H. B. Probst, MS 49-1
	National Aeronautics and Space Administration, Langley Research Center, Hampton, VA 23665
1	ATTN: Mr. J. Buckley, Mail Stop 387
	Department of Energy, Division of Transportation, 20 Massachusetts Avenue, N.W., Washington, DC 20545
1	ATTN: Mr. Robert Schultz (TEC)

No. of Copies	To
	National Bureau of Standards, Washington, DC 20234
1	ATTN: Dr. S. Wiederhorn
	National Research Council, National Materials Advisory Board, 2101 Constitution Avenue, Washington, DC 20418
1	ATTN: D. Groves
1	R. M. Spriggs
	Case Western Reserve University, Department of Metallurgy, Cleveland, OH 44106
1	ATTN: Prof. A. H. Heuer
	Norton Company, Worcester, MA 01606
1	ATTN: Dr. N. Ault
1	Dr. M. L. Torti
	Ceramatec, Incorporated, 163W 1700S, Salt Lake City, UT 84115
1	ATTN: Dr. R. A. Cutler
	University of California, Davis College of Engineering, Davis, CA 95616
1	ATTN: Dr. Z. Munir
1	Ms. K. Philpot
	Lawrence Livermore National Laboratory, P.O. Box 808, Livermore, CA 94550
1	ATTN: Dr. J. B. Holt
1	Dr. C. T. Chow
1	Dr. C. F. Cline
1	Dr. M. Wilkins
	Rice University, P.O. Box 2692, Houston, TX 77252
1	ATTN: Prof. J. Margrave
1	Dr. R. Hauge
1	Dr. L. Fredin
	Los Alamos National Laboratory, P.O. Box 1663, Los Alamos, NM 87545
1	ATTN: Dr. R. G. Behren; MST-3/MS-C348
1	Dr. K. Wylie; MS G780
1	Mr. R. Riley
1	Dr. R. Newkirk
1	Mr. D. J. Sandstrom
	System Planning Corporation, 1500 Wilson Boulevard, Arlington, VA 22209
1	ATTN: Mr. W. L. Frankhouser
	Sandia National Laboratories, Division 8363, Livermore, CA 94550
1	ATTN: Dr. S. B. Margoulis

No. of Copies	To
	Northwestern University, Department of Engineering Sciences and Applied Mathematics, Evanston, IL 60201
1	ATTN: Dr. B. J. Matkowsky
	Sandia National Laboratories, P.O. Box 5800, Albequerque, NM 87185
1	ATTN: Dr. R. A. Graham
	Georgia Tech Research Institute, Atlanta, GA 30332
1	ATTN: Ms. K. C. Logan
	Director, Army Materials and Mechanics Research Center, Arsenal Street, Watertown, MA 02172-0001
2	ATTN: AMXMR-PL
1	AMXMR-PR
1	AMXMR-K
1	AMXMR-OM, Dr. J. W. McCauley
10	Authors

Army Materials and Mechanics Research Center,
Watertown, Massachusetts 02172
SELF-PROPAGATING REACTIONS FOR SYNTHESIS OF HIGH TEMPERATURE MATERIALS
Peter D. Zavitsanos and Joseph F. D'Andrea
General Electric Company, RSD
3198 Chestnut Street
Philadelphia, PA 19101
Technical Report AMMRC TR-85-15
Contract No. DAAG46-83-C-0178
D/A Project: 1L263102D071
Final Report: Oct. 83 to Sept. 84

AD ____________
UNCLASSIFIED
LIMITED DISTRIBUTION

Key Words

Titanium powder, Boron powder, Titanium diboride, Synthesis, Heat of reaction, Density, Exothermic reactions, Titanium boride

This effort was undertaken to investigate the basic aspects of the condensed phase titanium-boron reaction leading to the formation of high density and quality TiB_2 under self-propagating conditions. Candidate factors for controlling microstructure were addressed and were utilized as variables in series of runs which produced TiB_2.

The heat of formation of TiB_2 was measured directly from the reacting elements in a modified bomb calorimeter; a $\Delta H^{\circ}_{f,298} = -71.01 \pm 1.9$ was determined which is sufficient to produce liquid TiB_2 under adiabatic conditions.

High density titanium diboride was prepared from elemental powders of titanium and boron through the self-propagation reaction process. By applying external pressure during the reaction period the product (TiB_2) has been densified to 95-97% theoretical density.

The microstructure and properties such as density, grain size, hardness, strength, toughness by indentation and modulus by elastic and sonic methods, are discussed as a function of variables such as starting stoichiometry, powder-particle size, mixing techniques and nucleation additives such as TiB_2 powder.

Army Materials and Mechanics Research Center,
Watertown, Massachusetts 02172
SELF-PROPAGATING REACTIONS FOR SYNTHESIS OF HIGH TEMPERATURE MATERIALS
Peter D. Zavitsanos and Joseph F. D'Andrea
General Electric Company, RSD
3198 Chestnut Street
Philadelphia, PA 19101
Technical Report AMMRC TR-85-15
Contract No. DAAG46-83-C-0178
D/A Project: 1L263102D071
Final Report: Oct. 83 to Sept. 84

AD ____________
UNCLASSIFIED
LIMITED DISTRIBUTION

Key Words

Titanium powder, Boron powder, Titanium diboride, Synthesis, Heat of reaction, Density, Exothermic reactions, Titanium boride

This effort was undertaken to investigate the basic aspects of the condensed phase titanium-boron reaction leading to the formation of high density and quality TiB_2 under self-propagating conditions. Candidate factors for controlling microstructure were addressed and were utilized as variables in series of runs which produced TiB_2.

The heat of formation of TiB_2 was measured directly from the reacting elements in a modified bomb calorimeter; a $\Delta H^{\circ}_{f,298} = -71.01 \pm 1.9$ was determined which is sufficient to produce liquid TiB_2 under adiabatic conditions.

High density titanium diboride was prepared from elemental powders of titanium and boron through the self-propagation reaction process. By applying external pressure during the reaction period the product (TiB_2) has been densified to 95-97% theoretical density.

The microstructure and properties such as density, grain size, hardness, strength, toughness by indentation and modulus by elastic and sonic methods, are discussed as a function of variables such as starting stoichiometry, powder-particle size, mixing techniques and nucleation additives such as TiB_2 powder.

Army Materials and Mechanics Research Center,
Watertown, Massachusetts 02172
SELF-PROPAGATING REACTIONS FOR SYNTHESIS OF HIGH TEMPERATURE MATERIALS
Peter D. Zavitsanos and Joseph F. D'Andrea
General Electric Company, RSD
3198 Chestnut Street
Philadelphia, PA 19101
Technical Report AMMRC TR-85-15
Contract No. DAAG46-83-C-0178
D/A Project: 1L263102D071
Final Report: Oct. 83 to Sept. 84

AD ____________
UNCLASSIFIED
LIMITED DISTRIBUTION

Key Words

Titanium powder, Boron powder, Titanium diboride, Synthesis, Heat of reaction, Density, Exothermic reactions, Titanium boride

This effort was undertaken to investigate the basic aspects of the condensed phase titanium-boron reaction leading to the formation of high density and quality TiB_2 under self-propagating conditions. Candidate factors for controlling microstructure were addressed and were utilized as variables in series of runs which produced TiB_2.

The heat of formation of TiB_2 was measured directly from the reacting elements in a modified bomb calorimeter; a $\Delta H^{\circ}_{f,298} = -71.01 \pm 1.9$ was determined which is sufficient to produce liquid TiB_2 under adiabatic conditions.

High density titanium diboride was prepared from elemental powders of titanium and boron through the self-propagation reaction process. By applying external pressure during the reaction period the product (TiB_2) has been densified to 95-97% theoretical density.

The microstructure and properties such as density, grain size, hardness, strength, toughness by indentation and modulus by elastic and sonic methods, are discussed as a function of variables such as starting stoichiometry, powder-particle size, mixing techniques and nucleation additives such as TiB_2 powder.

Army Materials and Mechanics Research Center,
Watertown, Massachusetts 02172
SELF-PROPAGATING REACTIONS FOR SYNTHESIS OF HIGH TEMPERATURE MATERIALS
Peter D. Zavitsanos and Joseph F. D'Andrea
General Electric Company, RSD
3198 Chestnut Street
Philadelphia, PA 19101
Technical Report AMMRC TR-85-15
Contract No. DAAG46-83-C-0178
D/A Project: 1L263102D071
Final Report: Oct. 83 to Sept. 84

AD ____________
UNCLASSIFIED
LIMITED DISTRIBUTION

Key Words

Titanium powder, Boron powder, Titanium diboride, Synthesis, Heat of reaction, Density, Exothermic reactions, Titanium boride

This effort was undertaken to investigate the basic aspects of the condensed phase titanium-boron reaction leading to the formation of high density and quality TiB_2 under self-propagating conditions. Candidate factors for controlling microstructure were addressed and were utilized as variables in series of runs which produced TiB_2.

The heat of formation of TiB_2 was measured directly from the reacting elements in a modified bomb calorimeter; a $\Delta H^{\circ}_{f,298} = -71.01 \pm 1.9$ was determined which is sufficient to produce liquid TiB_2 under adiabatic conditions.

High density titanium diboride was prepared from elemental powders of titanium and boron through the self-propagation reaction process. By applying external pressure during the reaction period the product (TiB_2) has been densified to 95-97% theoretical density.

The microstructure and properties such as density, grain size, hardness, strength, toughness by indentation and modulus by elastic and sonic methods, are discussed as a function of variables such as starting stoichiometry, powder-particle size, mixing techniques and nucleation additives such as TiB_2 powder.

Army Materials and Mechanics Research Center,
Watertown, Massachusetts 02172
SELF-PROPAGATING REACTIONS FOR SYNTHESIS OF HIGH TEMPERATURE MATERIALS
Peter D. Zavitsanos and Joseph F. D'Andrea
General Electric Company, RSD
3198 Chestnut Street
Philadelphia, PA 19101
Technical Report AMMRC TR-85-15
Contract No. DAAG46-83-C-0170
D/A Project: 1L263102D071
Final Report: Oct. 83 to Sept. 84

AD ______________
UNCLASSIFIED
LIMITED DISTRIBUTION

Key Words

Titanium powder, Boron powder, Titanium diboride, Synthesis, Heat of reaction, Density, Exothermic reactions, Titanium boride

This effort was undertaken to investigate the basic aspects of the condensed phase titanium-boron reaction leading to the formation of high density and quality TiB_2 under self-propagating conditions. Candidate factors for controlling microstructure were addressed and were utilized as variables in series of runs which produced TiB_2.

The heat of formation of TiB_2 was measured directly from the reacting elements in a modified bomb calorimeter; a $\Delta H_{f\,298}^{\circ} = -71.01 \pm 1.9$ was determined which is sufficient to produce liquid TiB_2 under adiabatic conditions.

High density titanium diboride was prepared from elemental powders of titanium and boron through the self-propagation reaction process. By applying external pressure during the reaction period the product (TiB_2) has been densified to 95-97% theoretical density.

The microstructure and properties such as density, grain size, hardness, strength, toughness by indentation and modulus by elastic and sonic methods, are discussed as a function of variables such as starting stoichiometry, powder-particle size, mixing techniques and nucleation additives such as TiB_2 powder.

Army Materials and Mechanics Research Center,
Watertown, Massachusetts 02172
SELF-PROPAGATING REACTIONS FOR SYNTHESIS OF HIGH TEMPERATURE MATERIALS
Peter D. Zavitsanos and Joseph F. D'Andrea
General Electric Company, RSD
3198 Chestnut Street
Philadelphia, PA 19101
Technical Report AMMRC TR-85-15
Contract No. DAAG46-83-C-0170
D/A Project: 1L263102D071
Final Report: Oct. 83 to Sept. 84

AD ______________
UNCLASSIFIED
LIMITED DISTRIBUTION

Key Words

Titanium powder, Boron powder, Titanium diboride, Synthesis, Heat of reaction, Density, Exothermic reactions, Titanium boride

This effort was undertaken to investigate the basic aspects of the condensed phase titanium-boron reaction leading to the formation of high density and quality TiB_2 under self-propagating conditions. Candidate factors for controlling microstructure were addressed and were utilized as variables in series of runs which produced TiB_2.

The heat of formation of TiB_2 was measured directly from the reacting elements in a modified bomb calorimeter; a $\Delta H_{f\,298}^{\circ} = -71.01 \pm 1.9$ was determined which is sufficient to produce liquid TiB_2 under adiabatic conditions.

High density titanium diboride was prepared from elemental powders of titanium and boron through the self-propagation reaction process. By applying external pressure during the reaction period the product (TiB_2) has been densified to 95-97% theoretical density.

The microstructure and properties such as density, grain size, hardness, strength, toughness by indentation and modulus by elastic and sonic methods, are discussed as a function of variables such as starting stoichiometry, powder-particle size, mixing techniques and nucleation additives such as TiB_2 powder.

Army Materials and Mechanics Research Center,
Watertown, Massachusetts 02172
SELF-PROPAGATING REACTIONS FOR SYNTHESIS OF HIGH TEMPERATURE MATERIALS
Peter D. Zavitsanos and Joseph F. D'Andrea
General Electric Company, RSD
3198 Chestnut Street
Philadelphia, PA 19101
Technical Report AMMRC TR-85-15
Contract No. DAAG46-83-C-0170
D/A Project: 1L263102D071
Final Report: Oct. 83 to Sept. 84

AD ______________
UNCLASSIFIED
LIMITED DISTRIBUTION

Key Words

Titanium powder, Boron powder, Titanium diboride, Synthesis, Heat of reaction, Density, Exothermic reactions, Titanium boride

This effort was undertaken to investigate the basic aspects of the condensed phase titanium-boron reaction leading to the formation of high density and quality TiB_2 under self-propagating conditions. Candidate factors for controlling microstructure were addressed and were utilized as variables in series of runs which produced TiB_2.

The heat of formation of TiB_2 was measured directly from the reacting elements in a modified bomb calorimeter; a $\Delta H_{f\,298}^{\circ} = -71.01 \pm 1.9$ was determined which is sufficient to produce liquid TiB_2 under adiabatic conditions.

High density titanium diboride was prepared from elemental powders of titanium and boron through the self-propagation reaction process. By applying external pressure during the reaction period the product (TiB_2) has been densified to 95-97% theoretical density.

The microstructure and properties such as density, grain size, hardness, strength, toughness by indentation and modulus by elastic and sonic methods, are discussed as a function of variables such as starting stoichiometry, powder-particle size, mixing techniques and nucleation additives such as TiB_2 powder.

Army Materials and Mechanics Research Center,
Watertown, Massachusetts 02172
SELF-PROPAGATING REACTIONS FOR SYNTHESIS OF HIGH TEMPERATURE MATERIALS
Peter D. Zavitsanos and Joseph F. D'Andrea
General Electric Company, RSD
3198 Chestnut Street
Philadelphia, PA 19101
Technical Report AMMRC TR-85-15
Contract No. DAAG46-83-C-0170
D/A Project: 1L263102D071
Final Report: Oct. 83 to Sept. 84

AD ______________
UNCLASSIFIED
LIMITED DISTRIBUTION

Key Words

Titanium powder, Boron powder, Titanium diboride, Synthesis, Heat of reaction, Density, Exothermic reactions, Titanium boride

This effort was undertaken to investigate the basic aspects of the condensed phase titanium-boron reaction leading to the formation of high density and quality TiB_2 under self-propagating conditions. Candidate factors for controlling microstructure were addressed and were utilized as variables in series of runs which produced TiB_2.

The heat of formation of TiB_2 was measured directly from the reacting elements in a modified bomb calorimeter; a $\Delta H_{f\,298}^{\circ} = -71.01 \pm 1.9$ was determined which is sufficient to produce liquid TiB_2 under adiabatic conditions.

High density titanium diboride was prepared from elemental powders of titanium and boron through the self-propagation reaction process. By applying external pressure during the reaction period the product (TiB_2) has been densified to 95-97% theoretical density.

The microstructure and properties such as density, grain size, hardness, strength, toughness by indentation and modulus by elastic and sonic methods, are discussed as a function of variables such as starting stoichiometry, powder-particle size, mixing techniques and nucleation additives such as TiB_2 powder.